

# **Environmental Security Technology Certification Program (ESTCP)**

## **Interim Report: Feature-based Detection and Discrimination at DuPont's Lake Success Business Park, Connecticut**

### **ESTCP Project #: UX-0210 Feature-based UXO Detection and Discrimination**



**January 2007  
Final – Revision 2**

Approved for public release: distribution is unlimited  
This research was supported wholly by the U.S. Department of Defense, through the Environmental Security Technology Certification Program (ESTCP) through Project 200210, under Contract DACA72-02-C-0033.

<b>REPORT DOCUMENTATION PAGE</b>				<i>Form Approved OMB No. 0704-0188</i>	
<small>The public reporting burden for this collection of information is estimated to average 1 hour per response, including the time for reviewing instructions, searching existing data sources, gathering and maintaining the data needed, and completing and reviewing the collection of information. Send comments regarding this burden estimate or any other aspect of this collection of information, including suggestions for reducing the burden, to the Department of Defense, Executive Services and Communications Directorate (0704-0188). Respondents should be aware that notwithstanding any other provision of law, no person shall be subject to any penalty for failing to comply with a collection of information if it does not display a currently valid OMB control number.</small>					
<b>PLEASE DO NOT RETURN YOUR FORM TO THE ABOVE ORGANIZATION.</b>					
<b>1. REPORT DATE (DD-MM-YYYY)</b>		<b>2. REPORT TYPE</b>		<b>3. DATES COVERED (From - To)</b>	
<b>4. TITLE AND SUBTITLE</b>				<b>5a. CONTRACT NUMBER</b>	
				<b>5b. GRANT NUMBER</b>	
				<b>5c. PROGRAM ELEMENT NUMBER</b>	
<b>6. AUTHOR(S)</b>				<b>5d. PROJECT NUMBER</b>	
				<b>5e. TASK NUMBER</b>	
				<b>5f. WORK UNIT NUMBER</b>	
<b>7. PERFORMING ORGANIZATION NAME(S) AND ADDRESS(ES)</b>				<b>8. PERFORMING ORGANIZATION REPORT NUMBER</b>	
<b>9. SPONSORING/MONITORING AGENCY NAME(S) AND ADDRESS(ES)</b>				<b>10. SPONSOR/MONITOR'S ACRONYM(S)</b>	
				<b>11. SPONSOR/MONITOR'S REPORT NUMBER(S)</b>	
<b>12. DISTRIBUTION/AVAILABILITY STATEMENT</b>					
<b>13. SUPPLEMENTARY NOTES</b>					
<b>14. ABSTRACT</b>					
<b>15. SUBJECT TERMS</b>					
<b>16. SECURITY CLASSIFICATION OF:</b>			<b>17. LIMITATION OF ABSTRACT</b>	<b>18. NUMBER OF PAGES</b>	<b>19a. NAME OF RESPONSIBLE PERSON</b>
a. REPORT	b. ABSTRACT	c. THIS PAGE			<b>19b. TELEPHONE NUMBER (Include area code)</b>

## Table of Contents

Table of Contents .....	i
Lists of Figures .....	iii
Lists of Tables .....	v
Acknowledgements .....	v
1. Introduction .....	1
1.1 Background .....	1
1.2 Objectives of the Demonstration .....	1
1.3 Regulatory Drivers .....	2
1.3.1 Regulatory Background Specific to Lake Success Business Park (LSBP) .....	3
1.4 Stakeholder/End-User Issues .....	3
2. Technology Description .....	4
2.1 Technology Developments and Application .....	4
2.1.1 UX-Analyze .....	4
2.1.2 Hardware .....	4
2.2 Previous Testing of the Technology .....	6
2.2.1 UX-Analyze .....	6
2.2.2 Characterization Modules .....	7
2.2.3 Classification Modules .....	11
2.2.4 Data Analysis Documentation .....	12
2.3 Factors Affecting Cost and Performance .....	13
2.4 Advantages and Limitations of the Technology .....	13
3. Demonstration Design .....	14
3.1 Performance Objectives .....	14
3.2 Selecting the Test Site .....	14
3.3 Test Site History/Characteristics .....	15
3.4 Present Operations .....	17
3.5 Pre-Demonstration Testing and Analysis .....	19
3.6 Testing and Evaluation Plan .....	20
3.6.1 Demonstration Set-up and Start-up .....	20
3.6.2 Period of Operation .....	21
3.6.3 Area Characterized .....	21
3.6.4 Demobilization .....	26
3.6.5 Data Processing Steps .....	26
4. Performance Assessment .....	27
4.1 Performance Criteria .....	27
4.2 Performance Confirmation Methods .....	27
4.3 Data Analysis, Interpretation, and Evaluation .....	27
4.3.1 Detection .....	27
4.3.2 Discrimination .....	34
4.3.3 Depth Estimates .....	44
4.3.4 Qualitative Metrics .....	46
4.4 Discussion .....	46

5. Cost Assessment .....	47
5.1 Cost Reporting .....	47
5.2 Cost Analysis .....	47
6. Implementation Issues .....	47
6.1 End User Issues.....	47
7. References.....	48
8. Points of Contact.....	49
ESTCP.....	49
SAIC .....	49
Dupont.....	49

## Lists of Figures

Figure 1. (Left) The standard EM61 / RTS pushcart configuration was modified for the DuPont survey by adding the low-metal IMU and lowering the prism height. (Right) Photograph of the pushcart magnetometer / RTS system.....	5
Figure 2. Screen snapshots showing UX-Analyze while selecting (or reviewing) individual anomalies. ....	7
Figure 3. Screen snapshots showing the user interface during data inversion. In this figure, the measured data is shown in the upper left map, the model parameters (fitted results) are displayed in the lower center window, and the forward model generated using the model parameters is shown in the upper right map. ....	8
Figure 4. Top – schematic showing the inclination and declination of the source objects. The inclination and declination range from 0 to 90 degrees in 15-degree increments. Bottom – synthesized electromagnetic and magnetic data, left and right respectively. Note the subtle changes in the shape of the anomalies for the various combinations of source dipole orientation. ....	9
Figure 5. Screen snapshots showing from left to right along each row (i) the segmentation of individual anomalies, (ii) the graphical interface used to identify and select individual anomalies, and (iii) anomaly-specific comparisons of measured and modeled data. Row (a) shows images for UX-Analyze EMI data, (b) DAS EMI, (c) UX-Analyze magnetic, and (d) DAS magnetic.....	10
Figure 6. Screen snapshots showing the user dialogue interfaces that call the classification routines.....	11
Figure 7. To document the analysis, UX-Analyze generates a one-page summary for each anomaly. In the anomaly summaries shown above, the measured data is shown in the upper left hand corner, the inverted model parameters in the middle left, the forward model in the upper rights, and a profile in the lower left corner. This layout was selected to provide insight into the confidence of the analysis and conclusions. EMI data for the anomaly are shown in the left summary, and magnetic data on the right. ....	12
Figure 8. DuPont’s Lake Success Business Park is located between Stratford and Bridgeport, CT. ....	16
Figure 9. Lake Success Business Park, the open forest region in the center of this satellite image, is located in an underdeveloped area of Bridgeport and Stratford, Connecticut. The development disparity with regards to the surrounding area is evident in this satellite image. ....	17
Figure 10. Left: Map showing the 70-acre grid boundaries and anomaly density (black circles) from the commercial contractor survey. The five-acre subset that is the area of interest for this demonstration is colored. Right: EM61 map of the five-acre area selected for this demonstration.....	19
Figure 11. Feature plot showing longitudinal versus transverse response coefficients for emplaced UXO types. The six data points per target represent distinct coil-UXO geometries. The contours are centered about the mean of the measurements and extend two standard deviations from the mean. ....	20
Figure 12. Site map showing the distribution of the emplaced ordnance on the five-acre site. ...	22

Figure 13. Site photographs - the top two photographs were taken prior to clearing the brush. The bottom two photographs were taken after brush clearing was completed in June 2004.	23
Figure 14. Coverage map showing the areas covered by EMI only, mag only, or both.....	24
Figure 15. Photographs of the two magnetometer platforms utilized during data acquisition. The pushcart system is shown in the left photo and the litter configuration on the right. ....	25
Figure 16. Site map showing magnetic coverage using the pushcart system (black symbols) and the litter configuration (blue). ....	25
Figure 17. Photographs taken during acquisition of EM61 MkII data using a template. The cued approach minimizes motion noise and errors in the spatial registration of the geophysical readings. ....	26
Figure 18. Color-coded map of the emplaced inert UXO items showing which were surveyed by Sky's magnetic system, EMI system, or both. ....	29
Figure 19. False color map showing the EMI data coverage overlain by locations of the emplaced targets and those declared detected during analysis. ....	30
Figure 20. False color map showing the magnetic data coverage overlain by locations of the emplaced targets and those declared detected during analysis. ....	31
Figure 21. Anomaly plots of two emplaced targets that were not picked as targets in the EMI data. Left Anomaly Plot – The location of a 105mm projectile is identified by the cross in the upper left map, but no signature is observed. Right Anomaly Plot – The location of a 57mm projectile is identified by the “X” in the upper left map. The ‘Comments’ field, which is located just above the profile in the two plots, reports the UXO type from the ground truth information. ....	32
Figure 22. Anomaly plots of two emplaced targets that were not picked as targets in the magnetic data. Left Anomaly Plot – The location of a 40mm projectile is identified by the cross in the upper left map. The spatial sampling pattern shown in the plot presumably resulted from trying to push and twist the pushcart through the grasses and cut debris. Right Anomaly Plot– The signature of a 57mm grenade, identified by the “X” in the upper left map, is within the background noise. The ‘Comments’ field, which is located just above the profile in the two plots, reports the UXO type from the ground truth information. ....	33
Figure 23. Scatter plot of the maximum signal versus dipole fit error. The data in this figure are restricted to emplaced UXO objects that were surveyed by Sky's production EM61 survey and the cued deployment. ....	34
Figure 24. Magnetic polarizability coefficients for emplaced targets, EM61 MkII data, gate 2. For the transverse coefficients plotted on the y-axis, symbols identify the mean of the two smaller magnetic response coefficients and lines show the range. ....	36
Figure 25. Photographs of native, non-emplaced objects for which data was acquired using a cued deployment and production survey. The photograph ID numbers correspond to those listed in Table 6. Although difficult to read, the top left photo is ID 87. ....	39
Figure 26. Receiver operating characteristic curves for cued data only. ....	40
Figure 27. Output from Duke's Support Vector Machine classifier; Sky's EM61 data. Each point represents the classifier value for an individual anomaly. The magenta symbols identify inert UXO items buried within the site which were used for calibration purposes. ....	42

Figure 28. Receiver operating characteristic curve for EMI classifications. The blue symbols plot Pd as a function of the number of false alarms. The red diamonds identify thresholds between rankings. ....	43
Figure 29. Scatter plot of the maximum signal versus dipole fit error for the test stand measurements, all cued targets (emplaced and non-emplaced), and all anomalies detected in Sky's EM61 MKII survey.....	44
Figure 30. Actual versus fitted depths for emplaced targets. Top: all seeded items, bottom: results for anomalies that possess fit errors of less than 0.22. ....	45

## **Lists of Tables**

Table 1. Comparison of Fitted Results using UX-Analyze and the DAS; magnetic data. ....	11
Table 2. Comparison of Fitted Results using UX-Analyze and the DAS; electromagnetic data. ....	11
Table 3. Performance Criteria.....	27
Table 4. Detection Performance by Ordnance Type and Sensor Modality .....	28
Table 5. Fit Results for Emplaced Targets; Cued vs. Sky Survey Data .....	37
Table 6. Fit Results for Native, Non-emplaced Targets; Cued vs. Sky Survey Data .....	38
Table 7. Fit Results for Emplaced Targets; Test Stand Data.....	41

## **Acknowledgements**

Contributing firms to this demonstration include SAIC, formally AETC Incorporated (lead), Duke University, and Sky Research. We thank Dr. Herb Nelson and others at the Naval Research Laboratory for supporting fieldwork associated with this work. We are beholden to DuPont for allowing us access to their property and genuinely thank Mr. Brian Ambrose, Mr. Scott Martin, and Mr. Rich Landis. This research was supported wholly by the U.S. Department of Defense, through the Environmental Security Technology Certification Program (ESTCP) through Project 200210, under Contract DACA72-02-C-0033.

## **Abstract**

The objective of this demonstration was to determine if laser-positioned, high-density EM61 data acquired in a moving survey mode could support feature-based discrimination decisions for a canopied site in Bridgeport Connecticut. Inversion results were benchmarked using cued data acquired in a controlled, gridded approach over 40 targets. In support of this effort, electromagnetic and magnetic data were acquired using man-portable sensor suites.

The geophysical data were spatially registered using a robotic total station because canopy at the site severely restricts the use of differential global positioning satellite systems. The pitch, roll and three-axis acceleration measurements of the sensors were measured using a low-metal inertial measurement unit. The survey site was seeded with inert UXO, ranging in size from 37mm to 105mm projectiles.

The feature-based EMI characterization approach demonstrated here inverts measured EM61 field data assuming a point dipole source and then segments the targets by feeding the inverted model parameters into statistical classifiers. We compared parameter estimates derived from both data sets and evaluated overall discrimination performances.

Results indicate that the laser-positioned EM61 data were not of sufficient quality to discriminate UXO from non-UXO. Of the 58 seeded items that were surveyed, 41 were ranked as high confidence ordnance, 10 were ranked as high confidence clutter, and 7 remained unclassified.



# Feature-based Detection and Discrimination at DuPont's Lake Success Business Park, Connecticut

## 1. Introduction

### 1.1 Background

With current technology and survey practices, unexploded ordnance (UXO) site characterization is inefficient and incomplete. Not all buried UXO are routinely detected, and UXO cannot be routinely distinguished from other items in the ground that pose no risk. Over the past five or six years, SERDP and ESTCP have invested heavily in developing survey data analysis and processing techniques for use with commercial sensors that can improve UXO detection and discrimination between UXO and clutter. These techniques include characterization procedures for estimating target features from survey data (size, shape, depth of burial, orientation, etc.) and feature-based classification procedures to aid decision-making.

Feature-based characterization and classification schemes have improved discrimination performance in some demonstrations. These algorithms, however, are not readily available to the user community and have had limited exposure to data acquired under 'production-imposed' constraints.

Our technical approach promotes the selection of potential UXO targets using quantitative evaluation criteria and transparent decision-making processes. In preparation of this demonstration, we developed an analysis framework within Oasis montaj™. The analysis algorithms provide quantitative evaluation criteria (e.g., target characterization and classification). Transparency is being achieved by leveraging the professional, flexible, and visual computing environment inherent in Oasis montaj™. Oasis montaj™ is a geophysical data processing and visualization package developed and marketed by Geosoft Incorporated. Oasis montaj™ has a large capacity database, a professional graphic interface, and an established client base.

### 1.2 Objectives of the Demonstration

The objective of this demonstration is to compare discrimination performance using laser-positioned, high-density EM61 data acquired in a moving survey mode with data acquired in a stationary grid (cued) approach for a canopied site, DuPont's Lake Success Business Park (LSBP), in Bridgeport Connecticut. Sky Research acquired electromagnetic and magnetic data using man-towed systems, one of which leverages work associated with SERDP program UX-1310 entitled 'Sensor Orientation Effects on UXO Geophysical Target Discrimination.' AETC Incorporated analyzed the data using UX-Analyze. Results from this Demonstration are compared and contrasted with baseline data including a survey conducted by a commercial contractor and data acquired in a cued fashion (viz., stationary sensor over fixed location).

### 1.3 Regulatory Drivers

The Senate Report (Report 106-50), pages 291–293, accompanying the *National Defense Authorization Act for Fiscal Year 2000* (Public Law 106-65), included a provision entitled “Research and development to support unexploded ordnance clearance, active range unexploded ordnance clearance, and explosive ordnance disposal.” This provision requires the Secretary of Defense to submit to the Congressional defense committees a report that gives a complete estimate of the current and projected costs, to include funding shortfalls, for UXO response at active facilities, installations subject to base realignment and closure (BRAC), and formerly used defense sites (FUDS).

The following statements are taken verbatim out of the DoDs 2001 Report to Congress:

*“Decades of military training, exercises, and testing of weapons systems has required that we begin to focus our response on the challenges of UXO. Land acreage potentially containing UXO has grown to include active military sites and land transferring or transferred for private use, such as Base Realignment and Closure (BRAC) sites and Formerly Used Defense Sites (FUDS). DoD responsibilities include protecting personnel and the public from explosive safety hazards; UXO site cleanup project management; ensuring compliance with federal, state, and local laws and environmental regulations; assumption of liability; and appropriate interactions with the public.*

*...Through limited experience gained in executing these activities, it has become increasingly clear that the full size and extent of the impact of sites containing UXO is yet to be realized. ... DoD has completed an initial baseline estimate for UXO remediation cost. This report provides a UXO response estimate in a range between \$106.9 billion and \$391 billion in current year [2001] dollars. ...Technology discovery, development, and commercialization offers some hope that the cost range can be decreased. ...*

*... **Objective: Develop standards and protocols** for navigation, geo-location, data acquisition and **processing**, and performance of UXO technologies.*

- Standard, high quality archived data are needed for optimal data processing of geophysical data, re-acquisition for response activities, quality assurance, quality control, and review by all stakeholders. In addition standards and protocols are required for evaluating UXO technology performance to aid in selecting the most effective technologies for individual sites.*
- **Standard software and visualization tools are needed to provide regulatory and public visibility to and understanding of the analysis and decision process made in response activities.***

### 1.3.1 Regulatory Background Specific to Lake Success Business Park (LSBP).

LSBP is an interim status Resource Conservation and Recovery Act (RCRA) facility. On August 21, 1990, Remington Arms Company, Inc. entered into an Administrative Consent Order (ACO) with USEPA. The ACO has been modified twice. The first modification (1994) authorized the construction of a Corrective Action Management Unit (CAMU), which is a facility designed to accumulate and treat contaminated soils. The second modification (1997) approved the implementation of Remedy I (excavation and treatment of upland soils).

A Phase I RCRA Facility Investigation (RFI) was performed in 1989-1991 and approved by EPA in 1992. Fifty-one Areas of Environmental Concern (AECs) were identified and investigated. The primary contaminant of concern is lead.

### 1.4 Stakeholder/End-User Issues

The stakeholders and end-users of this target characterization and classification technology include private contractors that conduct geophysical investigations in support of UXO clean up programs and governmental employees that provide technical oversight. DuPont is a key stakeholder. The demonstration of discrimination capabilities using survey data will significantly affect future clearance activities at the site.

## **2. Technology Description**

### **2.1 Technology Developments and Application**

This demonstration includes data acquisition and analysis components. The sensor system and platform are leveraged from SERDP project 1310 entitled ‘Sensor orientation effects on UXO geophysical target discrimination.’

#### **2.1.1 UX-Analyze**

Primary objectives of project UX-200210 are to transfer anomaly characterization and classification algorithms to the user community via Oasis montaj™ and to demonstrate the efficacy of the feature-based approach through multiple demonstrations at sites with a variety of near surface conditions and target objects. The anomaly characterization algorithms developed by AETC during the past decade assume a dipolar source and derive the best set of induced dipole model parameters that account for the spatial variation of the signal as the sensor is moved over the object. Algorithms for magnetic and electromagnetic induction (EMI) data have been developed and tested during previous demonstrations. The model parameters are target X,Y location and depth, three dipole response coefficients corresponding to the principle axes of the target (EMI only), and the three angles that describe the orientation of the target. The size of the target can be estimated using empirical relationships between either the dipole moment for magnetic data or the sum of the targets’ response coefficients. Cylindrical objects like most UXO have one large coefficient and two smaller, equal coefficients. Plate-like objects nominally have two large and one small coefficient.

UX-Analyze was developed during the first year of the program to facilitate efficient UXO data analysis within the Oasis montaj™ environment. It consists of multiple databases, custom graphical interfaces, and data visualizations. UX-Analyze provides the infrastructure to systematically identify and extract anomalies from the dataset, call the characterization routines, store the fitted source parameters for each anomaly, perform target classification, and document the analysis. Once the analysis is complete, individual images for each anomaly can be automatically produced for documentation purposes.

#### **2.1.2 Hardware**

Sky Research deployed a G-858 magnetometer, made by Geometrics, and an EM61 EMI system, made by Geonics Ltd., at the LSBP site (Figure 1). Four G-858 sensors were deployed using a rigid fiberglass push cart system. The EM61 was deployed using the standard wheel/coil configuration provided by Geonics. The magnetic and EM data were position-stamped with data collected from the Leica robotic total station (RTS). The orientation of the sensors during collection was measured using a low-metal inertial measurement unit (IMU) providing pitch, roll and 3-axis acceleration measurements.



Figure 1. (Left) The standard EM61 / RTS pushcart configuration was modified for the DuPont survey by adding the low-metal IMU and lowering the prism height. (Right) Photograph of the pushcart magnetometer / RTS system.

The following component technologies were used as part of the LSBP surveys.

- **Gyro:** RIS Corporation fabricated a low-metal IMU sensor for measurement of pitch, roll and three-axis acceleration. The unit has very low metal components. The unit has a built-in sensor that allows the measurement to be interleaved with the EM firing sequence. The gyro was housed in a fiberglass box and has plastic connectors. It has an on-board processor that will output ASCII information in the same format as the Crossbow IMU, which it replaced.
- **HipBox:** RIS Corp developed a multi-channel, asynchronous data logging unit called the Handheld Interface Pod, or HipBox. The HipBox logs the serial output stream of the G-858, EM61, gyro, RTS and GPS, stamps each recorded record with a time-tag, and produces a standard, concatenated ASCII serial output stream. The HipBox output stream is logged on a PC tablet for real-time data merging and data visualization.
- **RTS:** The Robotic Total Station is Leica model TSP1200, which replaced the TSP1100. The unit is a laser tracking system that provides real-time 3D positions at a rate of up to 8 HZ with sub-cm accuracy. The survey instrument, setup over a known point in the survey area, tracks a prism attached to the sensor system. The positional data is radioed to the roving system and fed into the HipBox as a serial stream.
- **Pushcart:** G-858 cesium-vapor sensors were deployed using a rigid fiberglass pushcart. The EM61 was deployed using two the standard wheel/coil configuration provided by Geonics (Figure 2-1, left).

The RIS HipBox was used to integrate all asynchronous serial sensor output; including, the (i) ASCII positional data from the Leica RTS 1200 at a rate of between 3 and 8 Hertz, (ii) binary serial output from the EM61 sensors, (iii) serial output at 10 Hz from the G-858 sensors, (iv) ASCII output from the low metal gyro at a rate of between 10 and 50 Hz, and (v) ASCII GPS output. The Trimble 5700 RTK GPS provides a 1 Hz solution.

The Leica robotic total station TSP1200 was used as the primary positioning system. The unit was mounted directly above the center of the EM61 coils. Two different prism mounting poles were used. First, a short pole was constructed that placed the prism 20 cm above the top EM61 coil. The short-pole has the advantage of creating a smaller lever-arm on the gimbaled EM coils, limiting sway. The short-pole has the disadvantage of limiting line-of-sight needed by the laser at all times due to operator obstruction. As such, the short-pole option was used only when the survey geometry allowed for “broadside” surveys, where the back-and-forth survey lines did not place the operator in an obstructing position. A long-pole configuration was also used, where the prism height is established above the operators head, thus avoiding line-of-sight issues. This configuration is less desirable as it exacerbates pendulum-like motions.

## **2.2 Previous Testing of the Technology**

We have performed preliminary tests of the Demonstration data analysis and classification technology during algorithm development. A number of the user graphical interfaces and dialogue boxes are briefly described below. Each of these capabilities have been tested individually and combined prior to submitting the Demonstration Plan.

### **2.2.1 UX-Analyze**

UX-Analyze allows users to systematically identify, extract, edit, and store data around individual anomalies. It provides efficient data structures and access for the analysis algorithms, stores the fitted parameters, and allows for multiple data types and surveys. This module is the interface between Oasis montaj™ and the Demonstration analysis software (Figure 2).

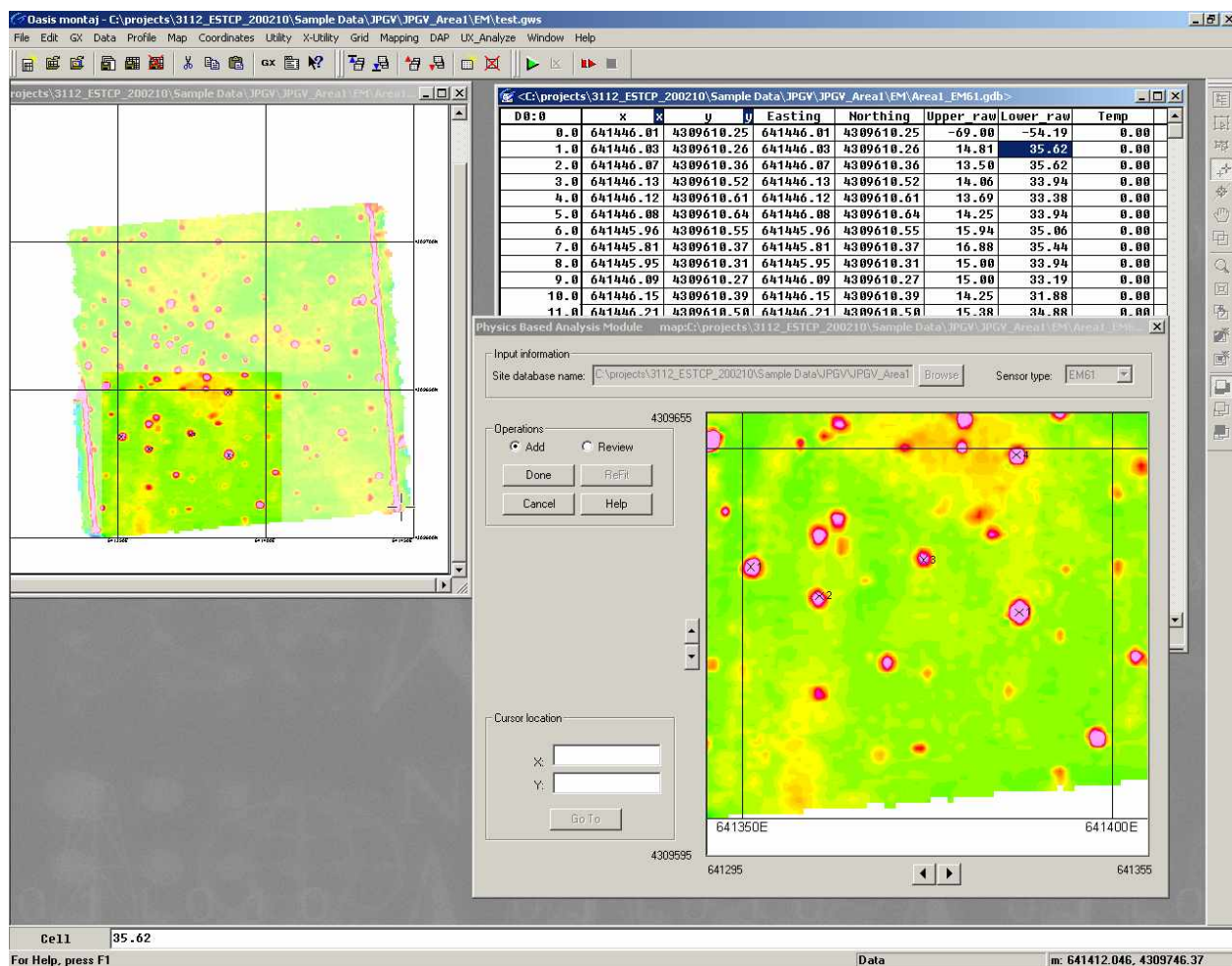


Figure 2. Screen snapshots showing UX-Analyze while selecting (or reviewing) individual anomalies.

## 2.2.2 Characterization Modules

Characterization routines for magnetic and EMI data have been integrated with UX-Analyze framework. These 3-D routines include graphic displays and controls that allow the user to manually select and filter the input data for each anomaly (Figure 3). The derived model parameters are stored in a master target database. The characterization modules, or inversion routines, were previously developed by AETC Incorporated for the *MTADS* Data Analysis System (DAS) under funding from ESTCP and SERDP (Barrow and Nelson, 1998; ESTCP Report 199526). The *MTADS* DAS codes were prototyped using the Interactive Data Language (IDL).

Algorithm equivalency tests verified that the C-based inversion routines embedded in Oasis montaj™ produce identical performances as the original formulations. Magnetic and EMI data



were synthesized for forty-nine sources that have a unique combination of inclination and declination but constant moment and depth of burial. The layout and noise-free synthetic data are shown in Figure 4 while Figure 5 shows screen snapshots of the user interfaces at various stages of the analysis process. To ensure that each routine received the exact same input for each anomaly, we extracted data samples around each anomaly individually once and then used the extracted data subsets as input for both. Source parameters were then calculated using the two inversion routines and shown to be equivalent for dipole inclinations of less than 75 degrees (Tables 1 and 2).

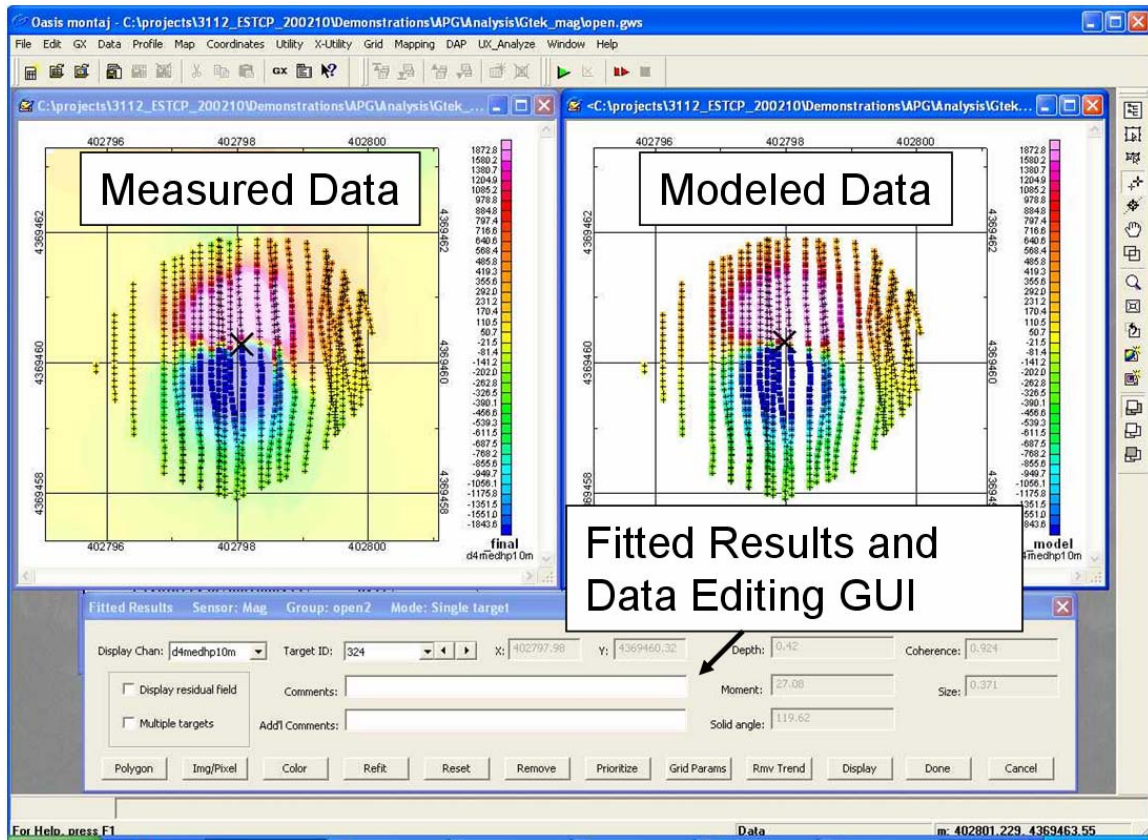


Figure 3. Screen snapshots showing the user interface during data inversion. In this figure, the measured data is shown in the upper left map, the model parameters (fitted results) are displayed in the lower center window, and the forward model generated using the model parameters is shown in the upper right map.



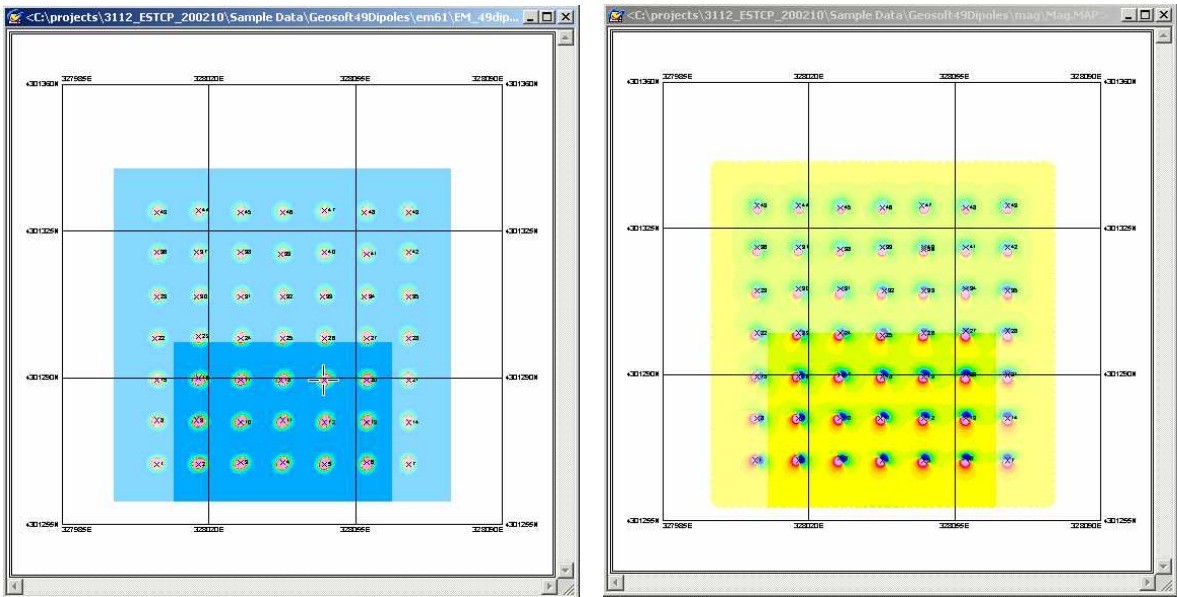
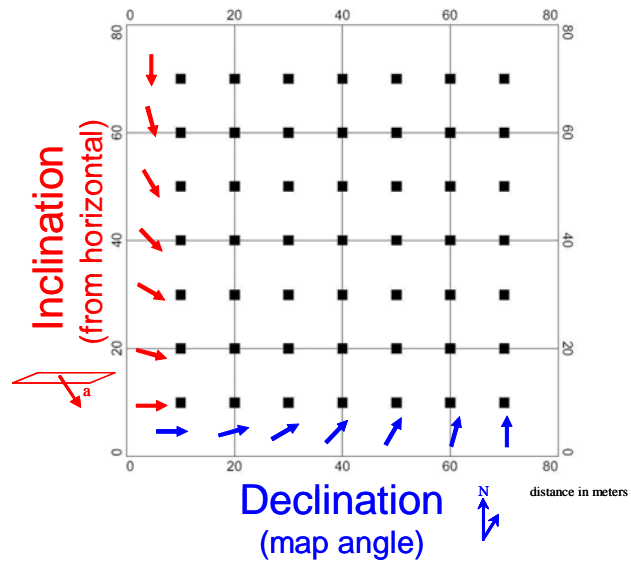


Figure 4. Top – schematic showing the inclination and declination of the source objects. The inclination and declination range from 0 to 90 degrees in 15-degree increments. Bottom – synthesized electromagnetic and magnetic data, left and right respectively. Note the subtle changes in the shape of the anomalies for the various combinations of source dipole orientation.

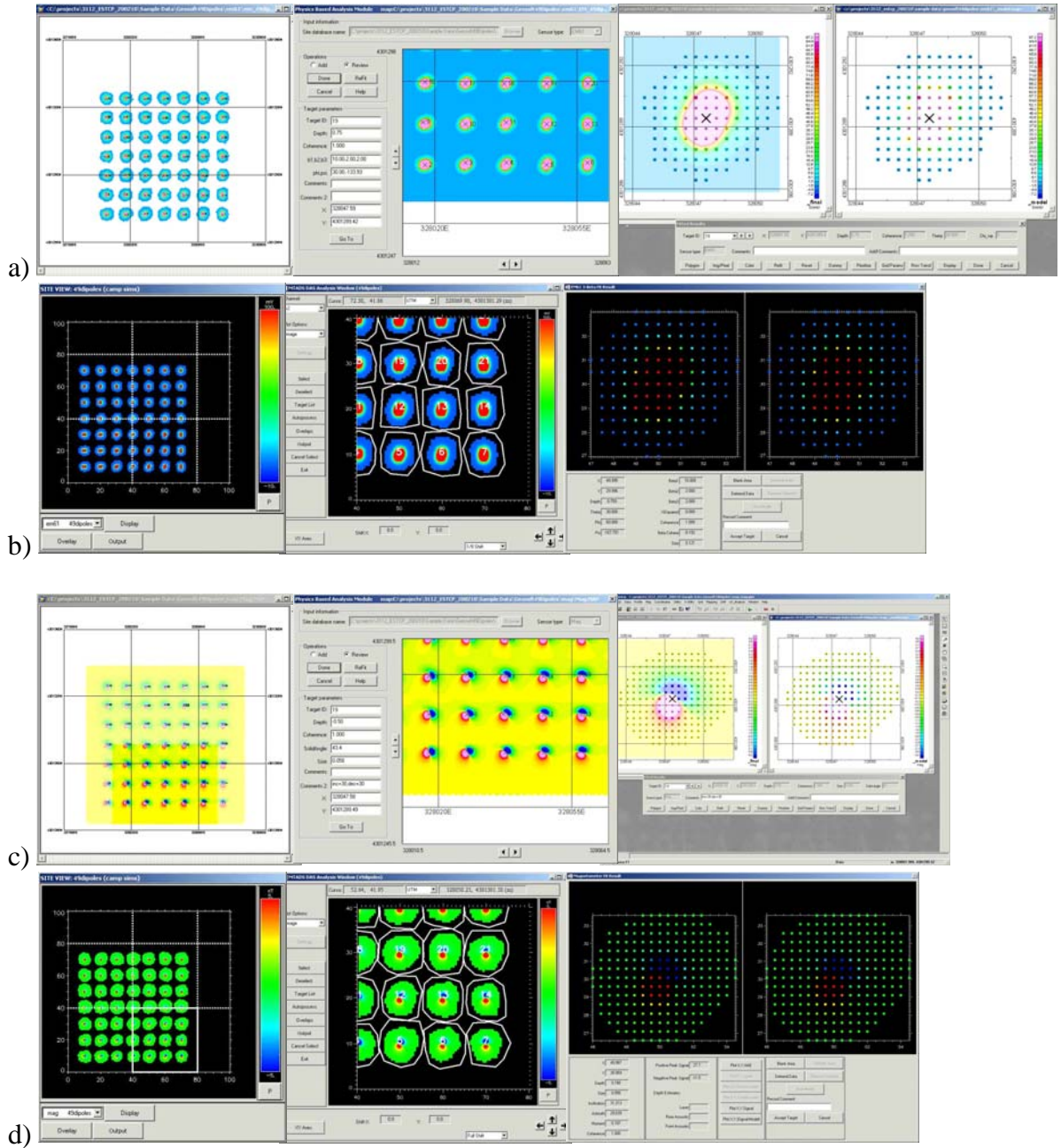


Figure 5. Screen snapshots showing from left to right along each row (i) the segmentation of individual anomalies, (ii) the graphical interface used to identify and select individual anomalies, and (iii) anomaly-specific comparisons of measured and modeled data. Row (a) shows images for UX-Analyze EMI data, (b) DAS EMI, (c) UX-Analyze magnetic, and (d) DAS magnetic.

Table 1. Comparison of Fitted Results using UX-Analyze and the DAS; magnetic data.

	X (m)	Y (m)	Depth (m)	Size (m)	Inc (deg)	Dec (deg)	Coherence
Average Difference	0.00	0.00	0.00	0.00	0.0	0.0	0.00
Standard Deviation	0.00	0.00	0.00	0.00	0.0	0.0	0.00

Table 2. Comparison of Fitted Results using UX-Analyze and the DAS; electromagnetic data.

	X (m)	Y (m)	Depth (m)	Dec (deg)	Inc (deg)	Beta1	Beta2	Beta3	Coherence
Average Difference	0.00	0.00	0.00	0.0	0.0	0.00	0.00	0.00	0.00
Standard Deviation	0.00	0.00	0.00	0.0	0.0	0.00	0.00	0.00	0.00

### 2.2.3 Classification Modules

Identifying objects as UXO or non-UXO based on estimated target features is notably difficult due to imperfect and non-unique feature estimates. The imperfect and non-unique feature estimates result largely from distortions in the spatial distribution of the anomaly. The distortions in turn are commonly caused by (i) errors in the spatial registration of the measured data samples, and/or (ii) nearby geologic or environmental signatures not associated with the source in question. As a result, separating the fitted parameters into distinct and disparate classes is non-trivial. Two classification methods that have proved promising during the past few years include the Generalized Likelihood Ratio Test and the Support Vector Machine. Dr. Leslie Collins, Duke University, and her colleagues have incorporated both classifiers into UX-Analyze as part of this program. The straightforward graphical user interface to these classifiers is shown in Figure 6.

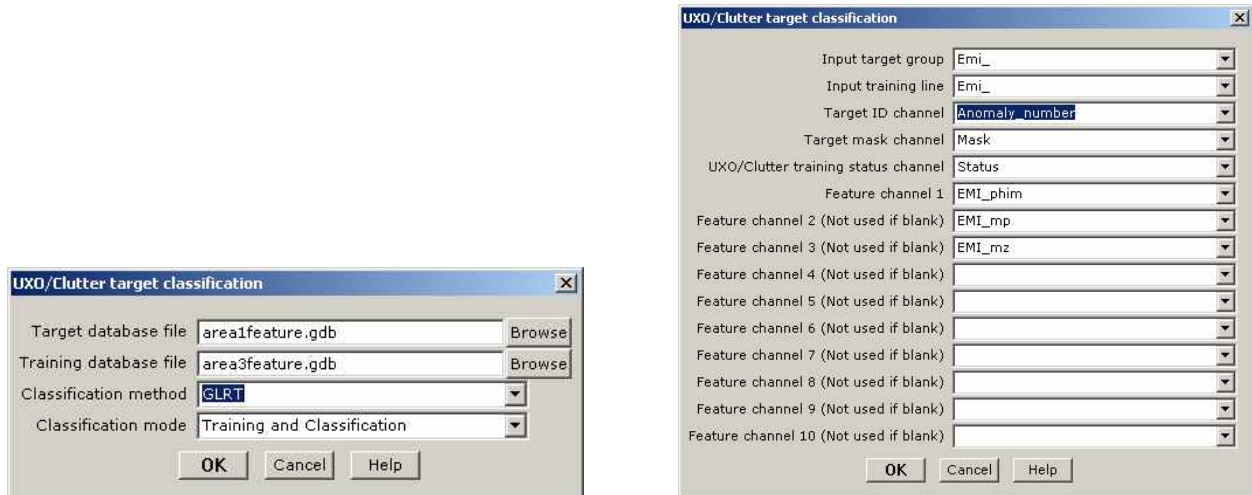


Figure 6. Screen snapshots showing the user dialogue interfaces that call the classification routines.

## 2.2.4 Data Analysis Documentation

UX-Analyze produces individualized anomaly reports, one for each anomaly, to document the decision process for each anomaly (Figure 7). In each plot, the measured data is graphically displayed next to the modeled data. The model parameters are listed in the middle of each page, and a profile extracted along the transect that passes closest to the fitted dipoles' location is located at the bottom. The positions of individual measurements are superimposed on the maps.

Essentially, the anomaly plots graphically provide an intuitive confidence measure. If the measured and modeled data are indistinguishable, the reviewer can have confidence that the estimated source parameters are approximately correct. If the two maps are do not resemble each other, however, it tells us that the source in question (i) cannot be represented well using a point dipole source, (ii) is not isolated, (iii) does not have sufficient signal-to-noise ratio, or (iv) was not properly sampled (spatially or temporally). In any case, if the two maps are dissimilar the inverted model parameters are most likely incorrect.

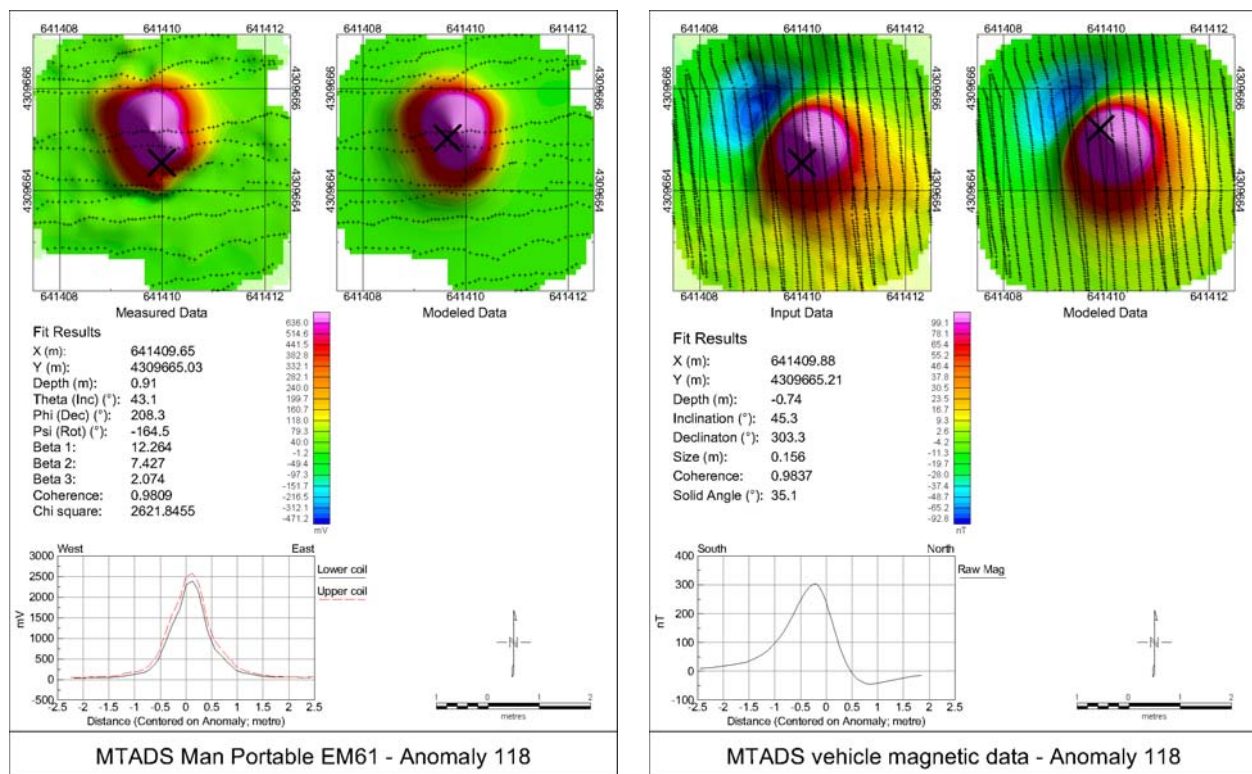


Figure 7. To document the analysis, UX-Analyze generates a one-page summary for each anomaly. In the anomaly summaries shown above, the measured data is shown in the upper left hand corner, the inverted model parameters in the middle left, the forward model in the upper right, and a profile in the lower left corner. This layout was selected to provide insight into the confidence of the analysis and conclusions. EMI data for the anomaly are shown in the left summary, and magnetic data on the right.

## **2.3 Factors Affecting Cost and Performance**

Costs to collect the data required by advanced processing are greater than that required for a detection survey. Higher acquisition cost result from data density, spatial registration, and signal to noise requirements that are necessary to support discrimination processing. In addition to higher field costs, more analysts' time is required for discrimination efforts compared to detection only objectives.

## **2.4 Advantages and Limitations of the Technology**

This demonstration technology uses spatially referenced geophysical data to estimate target parameters for each anomaly. The approach assumes a dipolar source. This has an inherent advantage over ad hoc analysis methods that are commonly used. Due to a lack of analysis routines available, many contractors make UXO and non-UXO declarations based on anomaly amplitude, half width, spatial footprint, or overall 'look'. These characterization methods are sensitive to the targets' orientation and depth of burial (or distance from the sensor). The methodology demonstrated here separates the measured signatures into that which is inherent to the target, and that which is related to the geometry of the problem (such as distance to sensor and orientation).

The primary advantage, therefore, is the potential for discriminating between UXO and non UXO-like objects based upon geophysical survey data. This is in contrast to simply identifying the location of anomalies from the geophysical survey data. Results from past demonstration have shown that that some discrimination is possible using magnetic and electromagnetic data (Robitaille et al., 1999). Magnetic discrimination is based primarily on the apparent fitted dipole moment (or apparent size if scaled correctly). Using EMI data, increased discrimination performance can sometimes be achieved by utilizing estimated shape information. If successful discrimination capabilities can be achieved, significant excavation savings can be realized by leaving the non-hazard clutter items unearthed.

This is not to say, however, that the technology being demonstrated will solve the UXO characterization and classification problems. Even with optimal data quality, the estimated fit parameters cannot always be separated into distinct, non-overlapping classes of UXO and non UXO-like objects. In addition, none of the fit parameters are actually unique to UXO items. Clutter items that physically resemble UXO will probably be misclassified. Additionally, if the data quality is not optimal the fitted parameters cannot be trusted.



### 3. Demonstration Design

#### 3.1 Performance Objectives

Type of Performance Objective	Primary Performance Criteria	Expected Performance (metric)	Actual Performance (all targets)
Quantitative	Analysis time	Characterize: <5 min/anomaly Document: <30 sec/anomaly	Characterize: 3min per anomaly Document: <15sec per anomaly
	% UXO Detected	>90	84
	% UXO Classified	>90	0.74
	False Negative	0	0.15
Qualitative	Ease of use	General Observations	See comments section 4.3.4
	Robustness	General Observations	See comments section 4.3.4

We ranked the classifier outputs using a scheme of 1, 2, and 3, where a rank of 1 indicates high confidence UXO, rank 3 is used for high confidence clutter, and rank 2 is everything else. The percentage UXO classified is defined as the Pd for rank 1 anomalies. The false negative metric is defined as those anomalies that are classified high confidence clutter, but were in fact UXO. It corresponds to (1-Pd) of the rank 3 anomalies.

#### 3.2 Selecting the Test Site

The demonstration site was selected because (i) there is a real and ongoing need to remediate the site in order to sell and develop the land, (ii) DuPont and AETC Incorporated have demonstrated past success utilizing cued data acquisition approaches, and (iii) advancements in laser ranging systems led us to believe that discrimination quality data (spatial registration precision at the centimeter level) could be acquired in lightly forested areas. The overarching financial motivation was to save monies by basing the discrimination decision on field survey data instead of cued data.

Two site visits were conducted prior to selecting the site and requesting approval from the ESTCP Program Office. Present at the initial meeting were R. Mehl, Sky Research, D. Keiswetter, AETC Incorporated, and B. Ambrose, DuPont. At the initial meeting, B. Ambrose identified a portion of DuPont's site for the demonstration so that Sky Research could to assess the feasibility of successfully deploying their hardware at this locale. Present at the second site walkover, which was conducted to confirm the suitability of the five-acre down select, were J. Foley, Sky Research, T. Bell, AETC Incorporated, and B. Ambrose.

### 3.3 Test Site History/Characteristics

Lake Success Business Park (LSBP) is a 422-acre underdeveloped industrial property located in Bridgeport and Stratford, Connecticut (Figure 8). Remington Arms Company, Inc. has owned the site the late 1800's. Remington manufactured, tested and stored small-caliber and other ammunition at the site. After the Vietnam War, site operations scaled back and the facility eventually ceased production in 1989. E. I. duPont de Nemours & Co. (DuPont) divested all operating Remington Arms facilities in 1993, but retained ownership of the closed Bridgeport/Stratford site. The Remington Arms name was transferred with the sale of the operating facilities. Remington Arms was renamed Sporting Goods Properties, Inc. (SGPI) and remains a subsidiary of DuPont. The site, formerly know as Remington Park or Remington Woods, was renamed Lake Success Business Park. Since 1989, 177 buildings containing asbestos and residual explosive materials have been demolished. The site is presently engaged in an aggressive remediation program. DuPont has received the approvals of the regulatory agencies to proceed with redevelopment of this parcel (Figure 9). During remediation of areas of environmental concern at other locations on LSBP both small and large caliber munitions were found in places where they were not expected. As an added precaution prior to releasing this portion of the site for redevelopment DuPont wants to conduct UXO survey utilizing current state of the art detection and mapping technologies and field verification to determine if UXOs are present.

LSBP is an interim status Resource Conservation and Recovery Act (RCRA) facility. On August 21, 1990, Remington Arms Company, Inc. entered into an Administrative Consent Order (ACO) with USEPA. The ACO has been modified twice. The first modification (1994) authorized the construction of a Corrective Action Management Unit, which is a facility designed to accumulate and treat contaminated soils. The second modification (1997) approved the implementation of Remedy I (excavation and treatment of upland soils). A Phase I RCRA Facility Investigation was performed in 1989-91 and approved by EPA in 1992. Fifty-one areas of environmental concern were identified and investigated. The primary contaminant is lead.

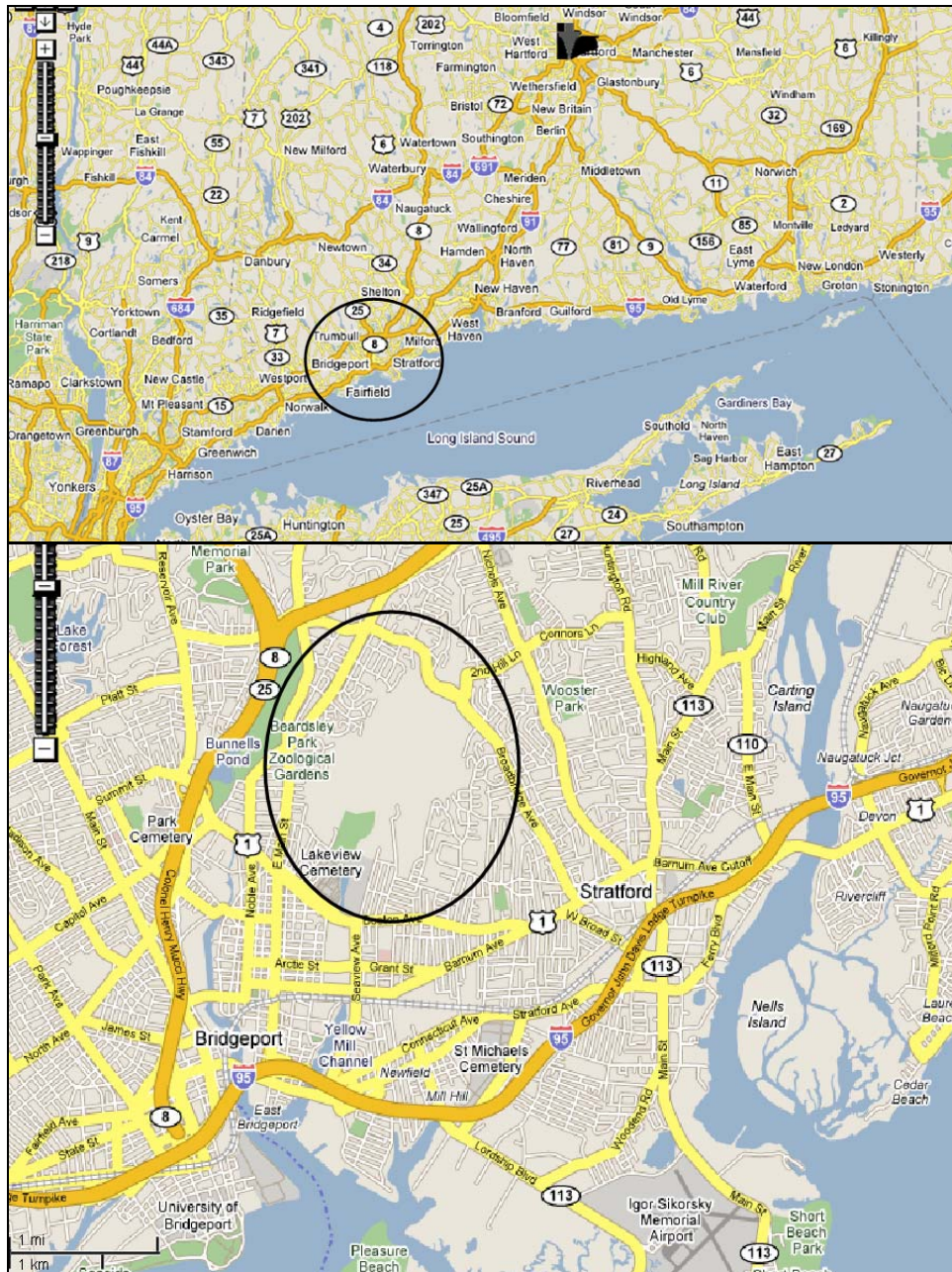


Figure 8. DuPont's Lake Success Business Park is located between Stratford and Bridgeport, CT.





Figure 9. Lake Success Business Park, the open forest region in the center of this satellite image, is located in an underdeveloped area of Bridgeport and Stratford, Connecticut. The development disparity with regards to the surrounding area is evident in this satellite image.

### **3.4 Present Operations**

During 2000 and 2001, DuPont hired a commercial contractor to survey seventy acres of the LSBP site. This acreage was selected because of its priority in the transition process. As a result of the survey, over 2,100 anomalies were identified (Figure 10). The data quality and density did not support advanced analysis. An intrusive investigation of approximately 300 anomalies in a four-acre portion of the site yielded a plethora of wire items and metallic debris, a significant number of ‘no finds’, and no ordnance items. Aside from the excavation within four-acre parcel, no subsequent action has occurred within the original boundaries of the 70-acre investigation area. The five-acre parcel associated with this Demonstration is within the original 70-acre survey.

In 2002 DuPont contracted AETC Incorporated to conduct a digital geophysical mapping survey to identify potential UXOs over an 18-acre parcel in the southwestern corner of LSBP. The 18-acre parcel was not included in the prior 70-acre survey. This acreage was also selected in response to transition plans and schedules. DuPont’s objective was to render clean the 18-acre parcel in Bridgeport. Prior to surveying the 18 acres, a test bed containing a number of 37mm, 47mm and 75mm surrogates buried at various depths and orientations as well as various clutter items was established and surveyed in August 2002. The test bed was surveyed with a GEM-3, an EM61 Mark 2 (EM61) and a SmartMag magnetometer. Based on the results of the test bed surveys the EM61 MKII was selected for the 18-acre parcel.

In March 2003, AETC reported approximately 1800 anomalies in the 18-acre parcel. Each anomaly was categorized as (1) possible UXO, (2) uncertain / more information needed, or (3)

high confidence not UXO. This effort essentially focused on reducing costs by identifying those anomalies that were not UXO; 852 of 1,546 contacts were ruled out based on the analysis of EM61 MKII survey data. Each of the remaining 694 anomalies was relocated and surveyed using an EM61-HH sensor in a cued mode. The priorities were then reassigned based on EM61-HH processing for each of the 694 anomalies. This process eliminated 584 (84%) of the 694 potential UXO contacts using feature-based analysis of the EM61-HH cued data. The remaining 110 anomalies were targeted for intrusively investigated. In the fall of 2003 all but 40 of the anomalies were investigated. No UXO were found. The cost savings on excavation and blast containment is estimated at \$1 million (Ambrose, 2004). The expenditures for the EM61-HH data collection and discrimination processing were \$45k and \$35k respectively.

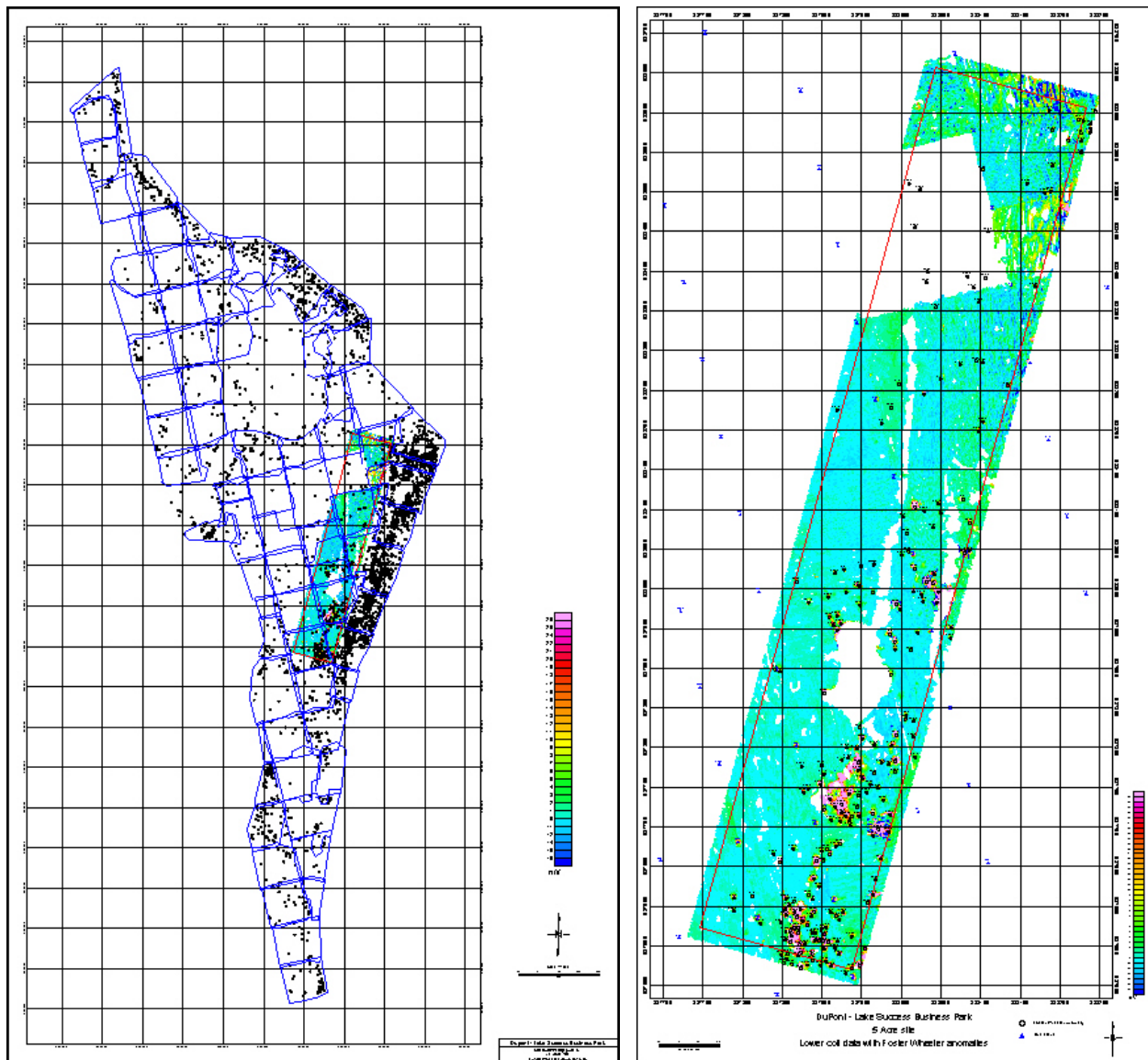


Figure 10. Left: Map showing the 70-acre grid boundaries and anomaly density (black circles) from the commercial contractor survey. The five-acre subset that is the area of interest for this demonstration is colored. Right: EM61 map of the five-acre area selected for this demonstration.

### 3.5 Pre-Demonstration Testing and Analysis

Calibration data were acquired for a variety of ordnance objects prior to the start of field work. Anecdotal evidence indicated that munitions including 37mm, 40mm, 57mm, 60mm, 105mm and 2.75in mortars may be present. Because no recovered inert ordnance at the site existed, we utilized inert UXOs provided by the Army Environmental Center. EM61 MkII data were

acquired in controlled tests using the same sensor that would be used for production work. Data were taken for each ordnance item in six orientations. The orientations were nose-up, nose-down, horizontal in X, horizontal in Y, 45 degree nose-up, and 45 degree nose-down. The sensor coils were horizontal as shown below.

Figure 11 shows the recovered longitudinal versus transverse response coefficients. There are six data point per ordnance type (one for each sensor-UXO configuration; nose-up, nose-down, horizontal in X, horizontal in Y, 45 degree nose-up, and 45 degree nose-down). The contours encircle an area that is two times the standard deviation about the mean for each ordnance type.

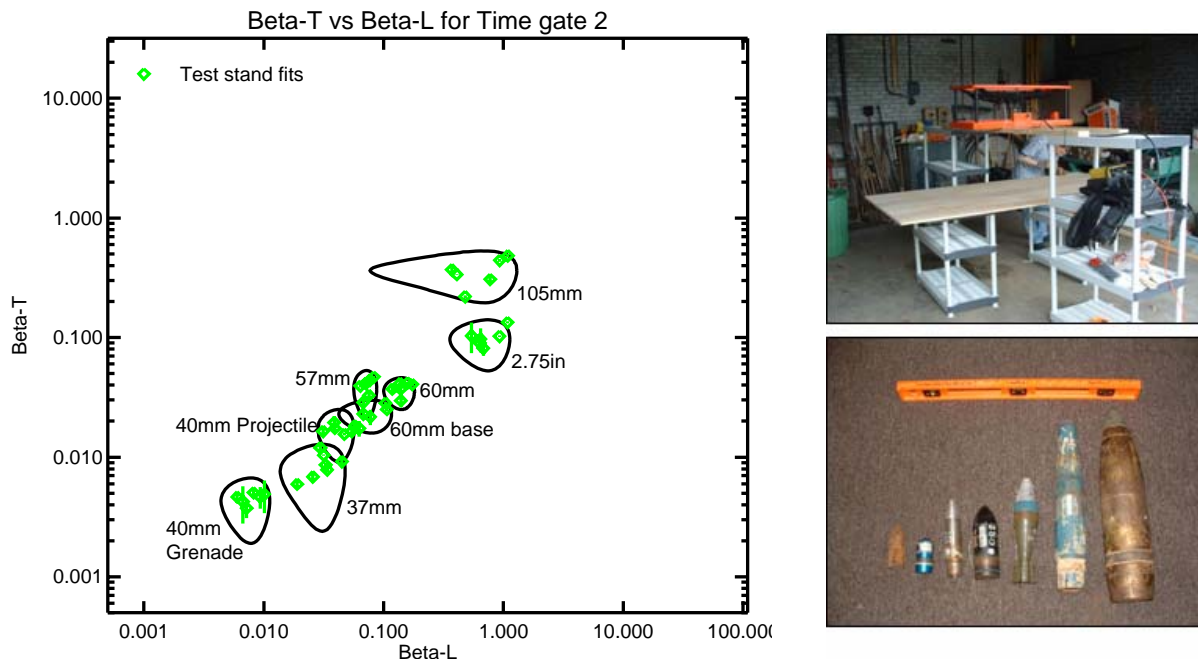


Figure 11. Feature plot showing longitudinal versus transverse response coefficients for emplaced UXO types. The six data points per target represent distinct coil-UXO geometries. The contours are centered about the mean of the measurements and extend two standard deviations from the mean.

### 3.6 Testing and Evaluation Plan

#### 3.6.1 Demonstration Set-up and Start-up

Inert ordnance from the Aberdeen Test Center (ATC) APG MD was seeded within the survey area to ensure the presence of UXO. ATC degaussed the ordnance and transferred it to Connecticut for emplacement on the site. Mr. Brian Ambrose and Mr. Jeffrey Fairbanks, HydroGeoLogic, Inc. emplaced the ordnance. The ground truth for the seeded targets was held until after the completion of the survey - it was not available to any data analyst associated with this project until the completion of their assigned analyses. The location of the emplaced

ordnance is shown in Figure 12. The emplaced ordnance types included 37mm projectiles, 40mm grenades, 40mm projectiles, 57mm projectiles, 60mm mortars 105mm projectiles, and 2.75inch rockets. The ordnance was buried at depths shallower than eleven times their diameter.

DuPont paid for and oversaw brush clearing activities during May 2004. Photographs of the site before and after clearance activities are shown in Figure 13.

### 3.6.2 Period of Operation

Sky Research acquired EMI and magnetic data during June 2004. Sky Research mobilized the field crew to the site on June 1 and demobilized Tuesday June 22.

### 3.6.3 Area Characterized

Sky Research surveyed an area that was 0.83 hectare (2.0 acres) in size using the EM sensor system and 0.95 hectare (2.4 acres) using the magnetic system (Figure 14).

Magnetic data were acquired using two different platforms, a pushcart and litter configuration. Photographs of the two systems are shown in Figures 15 while the coverage is shown in Figure 16. Because of its design, the pushcart platform had difficulty operating in grasses, short brush stubble, and crossing tire ruts or surface debris. A litter configuration was constructed and utilized June 9.

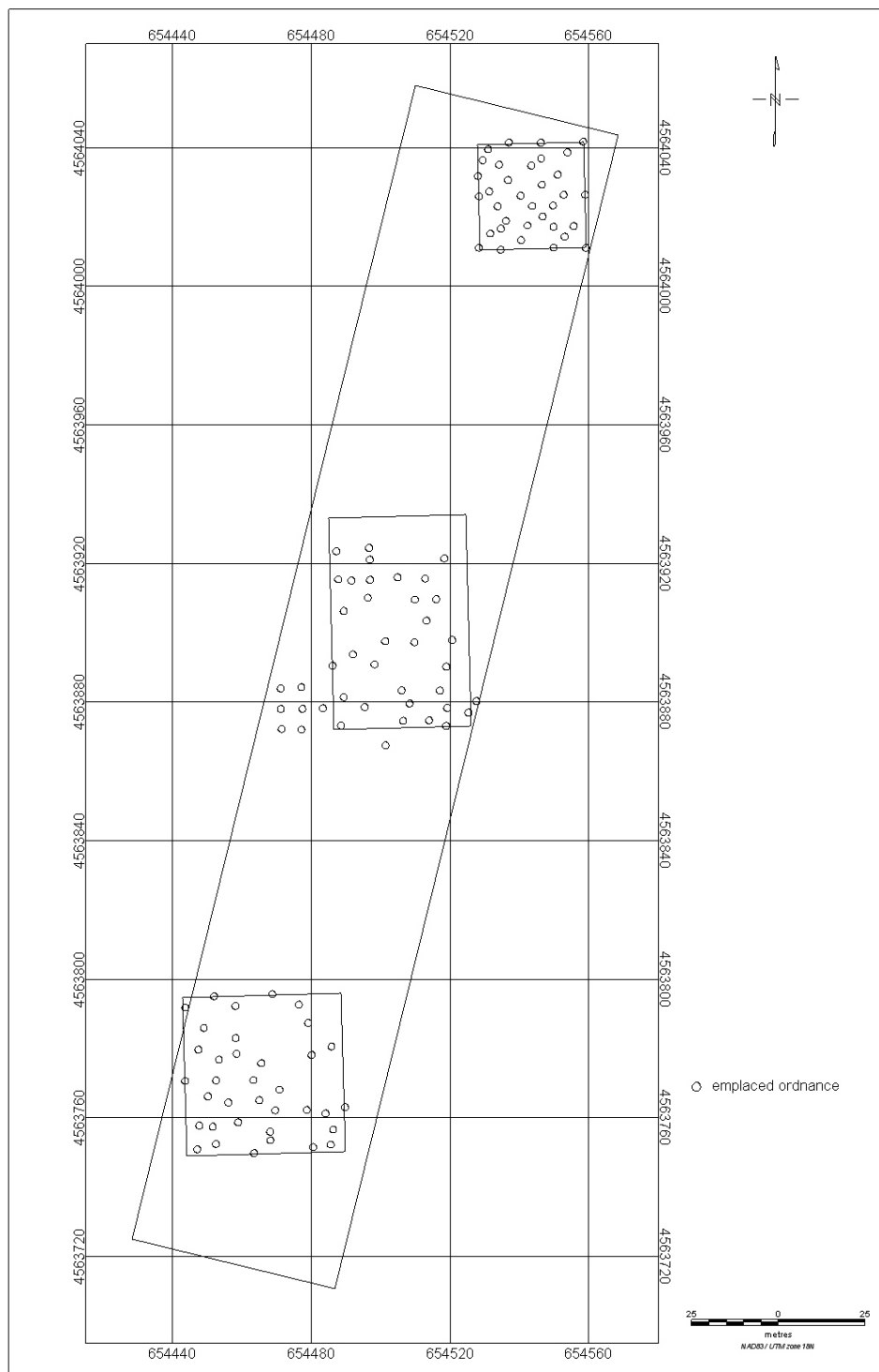


Figure 12. Site map showing the distribution of the emplaced ordnance on the five-acre site.





Figure 13. Site photographs - the top two photographs were taken prior to clearing the brush. The bottom two photographs were taken after brush clearing was completed in June 2004.

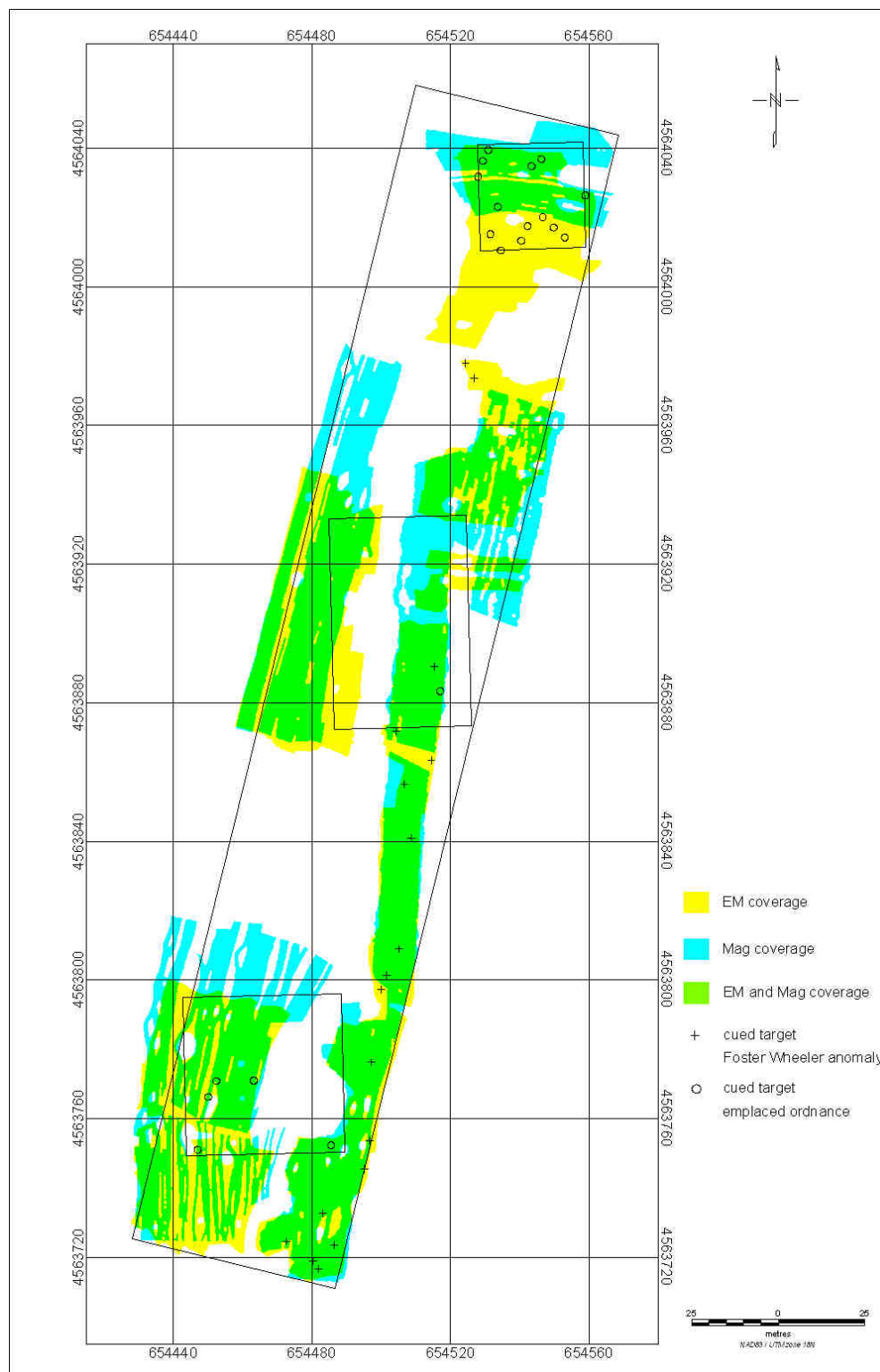


Figure 14. Coverage map showing the areas covered by EMI only, mag only, or both.





Figure 15. Photographs of the two magnetometer platforms utilized during data acquisition. The pushcart system is shown in the left photo and the litter configuration on the right.

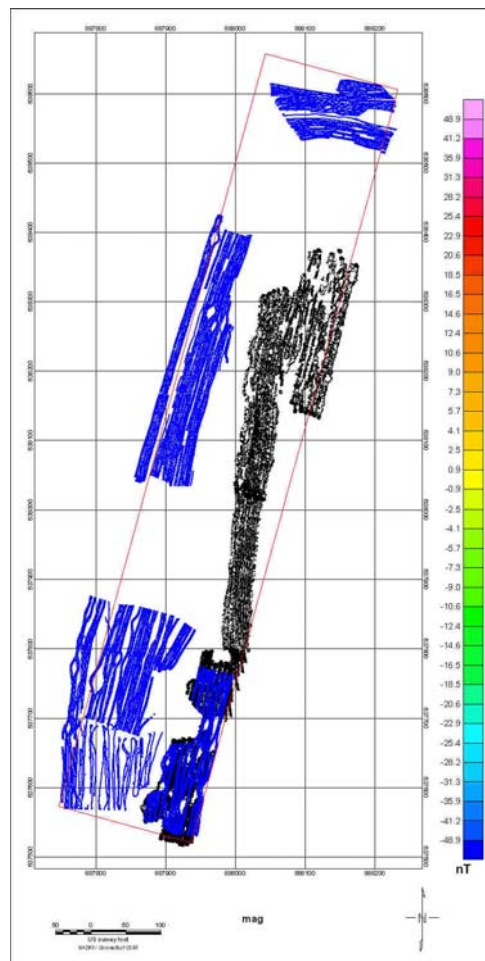


Figure 16. Site map showing magnetic coverage using the pushcart system (black symbols) and the litter configuration (blue).

In addition to the production survey data, EM61 MKII data were acquired in a grid over twenty emplaced targets and twenty anomalies identified in the original Foster-Wheeler survey data (Figure 17). Collecting data in a static grid configuration minimizes errors in positioning that area associated with survey motion. The cued data were collected on a 6x5 point rectangle grid (nodes separated by 20.3cm [8inches] and 40.6cm [16inches] respectively resulting in a 101.5x162.4cm [3¼ - x 5¼-foot] area). The grid was elevated 20 cm above the ground, and the EM61 was positioned directly on the grid nodes, without wheels. Sensor locations on the grid were controlled by lining up cross hairs on the EM61 bottom coil with grid line intersections. The choice of grid layout and elevation was based on results of simulations of data inversion sensitivity.



Figure 17. Photographs taken during acquisition of EM61 MkII data using a template. The cued approach minimizes motion noise and errors in the spatial registration of the geophysical readings.

#### 3.6.4 Demobilization

At the conclusion of the survey, all Sky Research equipment was packed and transported to a commercial shipping company.

#### 3.6.5 Data Processing Steps

As mentioned above in section 2.1.2, all sensor and spatial registration data were read into the HipBox as asynchronous serial records. When received, the HipBox stamps each incoming record with the HipBox time, reformats each data record, and concatenates the various data into a multiplexed output stream. In terms of serial input data, the HipBox acts as a data accumulator, reformatting and time-stamping all input data. Once all data are reformatted and brought to a common time-base, the data are logged on a tablet PC using a customized data logging program; RisLogger. This program provides several data manipulation, merging, and visualization functions. One essential task in the data merging is the establishment of the position of each sensor reading (sensor value and time) based on the data provided by the RTS (prism position and time). This is done for G-858, EM61 and gyro data.

## 4. Performance Assessment

### 4.1 Performance Criteria

Table 3. Performance Criteria

Performance Criterion	Description	Primary or Secondary
Analysis Time	Times required making a decision for each anomaly and prepare required documentation supporting the decision. Analysis time will be logged into two categories: A) identifying, characterizing, and classifying individual anomalies, and B) preparing anomaly specific images and dig sheet information.	Primary
% UXO Detected	(# of detections at emplaced ordnance locations)/(# of emplaced ordnance)	Primary
% UXO Classified	(# of anomalies that are classified as a priority 1)/(# of actual ordnance found)	Primary
# False Negatives	Anomaly classified as high confidence clutter (priority 3) that is actually a UXO	Primary
Ease of Use	Describe the processing flow and the anticipated skill level required. Although the data analysts working on this demonstration are not novices with regard to UX-Analyze, the goal of the program is that data processors experienced with Oasis montaj™ could utilize the software with the on-line help and without hands-on training.	Primary
Robustness	No major bugs that artificially limit the analysts' ability to conduct analysis.	Primary

### 4.2 Performance Confirmation Methods

The Sky Research magnetic and EMI systems surveyed portions of the site in which the ESTCP Program Office arranged for a variety of inert ordnance to be seeded. After analysis of the data, we submitted target lists to the Program Office. Using the known positions of these emplaced targets, the detection and discrimination performance was calculated.

### 4.3 Data Analysis, Interpretation, and Evaluation

#### 4.3.1 Detection

The emplaced targets can be utilized to assess the detection performance because we know their number and locations. The ESTCP Program Office arranged for 102 inert UXO items to be

emplaced within the 5-acre area. The emplaced items included 7 105mm projectiles, 17 2.75-inch warheads, 17 60mm projectiles, 16 57mm projectiles, 21 40mm grenades, 21 40mm projectiles, and 3 37mm projectiles. In addition, one of each ordnance type was buried within the survey grid to serve as calibration targets. The locations and details of the seven calibration targets were provided to Sky Research personnel for system performance tests.

Not all of the emplaced targets were surveyed by Sky's EMI sensor or by their magnetic systems. Figure 18 is color-coded to show which instrument surveyed each of the emplaced targets. Of the 102 emplaced targets, only 69 targets were surveyed by Sky's EMI system and 60 by their magnetic systems (Figures 19 and 20).

Of the 69 emplaced targets surveyed with the EMI sensor, 58 were selected as potential objects, resulting in 84% detection rate. Of the eleven emplaced items that were not picked as targets in the EMI data, three had data problems and eight were at or below background noise levels. The majority of the missed targets were 40mm projectiles or grenades. Excluding the 40mm projectiles and grenades, one 105mm projectile and two 57mm mortars were not detected. Figure 21 shows the 105mm and one of the 57mm projectiles that were not picked at the emplaced targets' location. Table 4 summarizes the detection results by ordnance type and sensor.

Of the 50 emplaced, ferrous targets surveyed with the magnetic sensors, 33 were selected as potential targets, resulting in 66% UXO detection rating. Half of the missed targets were 40mm or 57mm projectiles. Figure 22 provides examples of emplaced targets for which an anomaly was not detected and declared.

Table 4. Detection Performance by Ordnance Type and Sensor Modality

Item	Total	EMI		Mag	
		Surveyed	Detected	Surveyed	Detected
37mm Projectile	3	2	2	1	0
40mm Grenade**	21	15	8	10	1
40mm Projectile	21	12	11	8	4
57mm Projectile	17	9	7	13	6
60mm Mortar	18	11	11	11	8
2.75" Rocket	17	14	14	11	10
105mm Projectile	7	6	5	6	5

\*\* non-ferrous

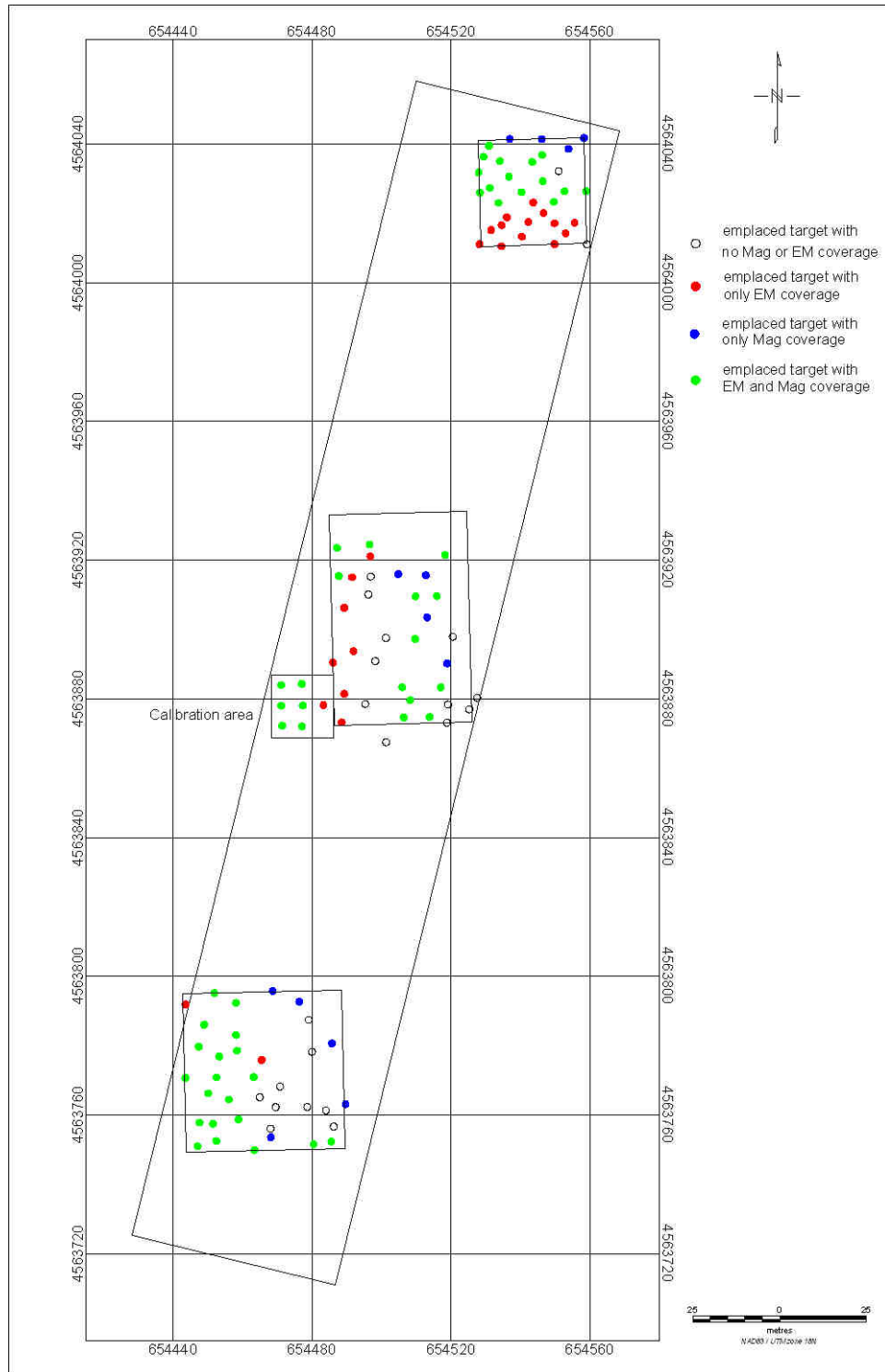


Figure 18. Color-coded map of the emplaced inert UXO items showing which were surveyed by Sky's magnetic system, EMI system, or both.



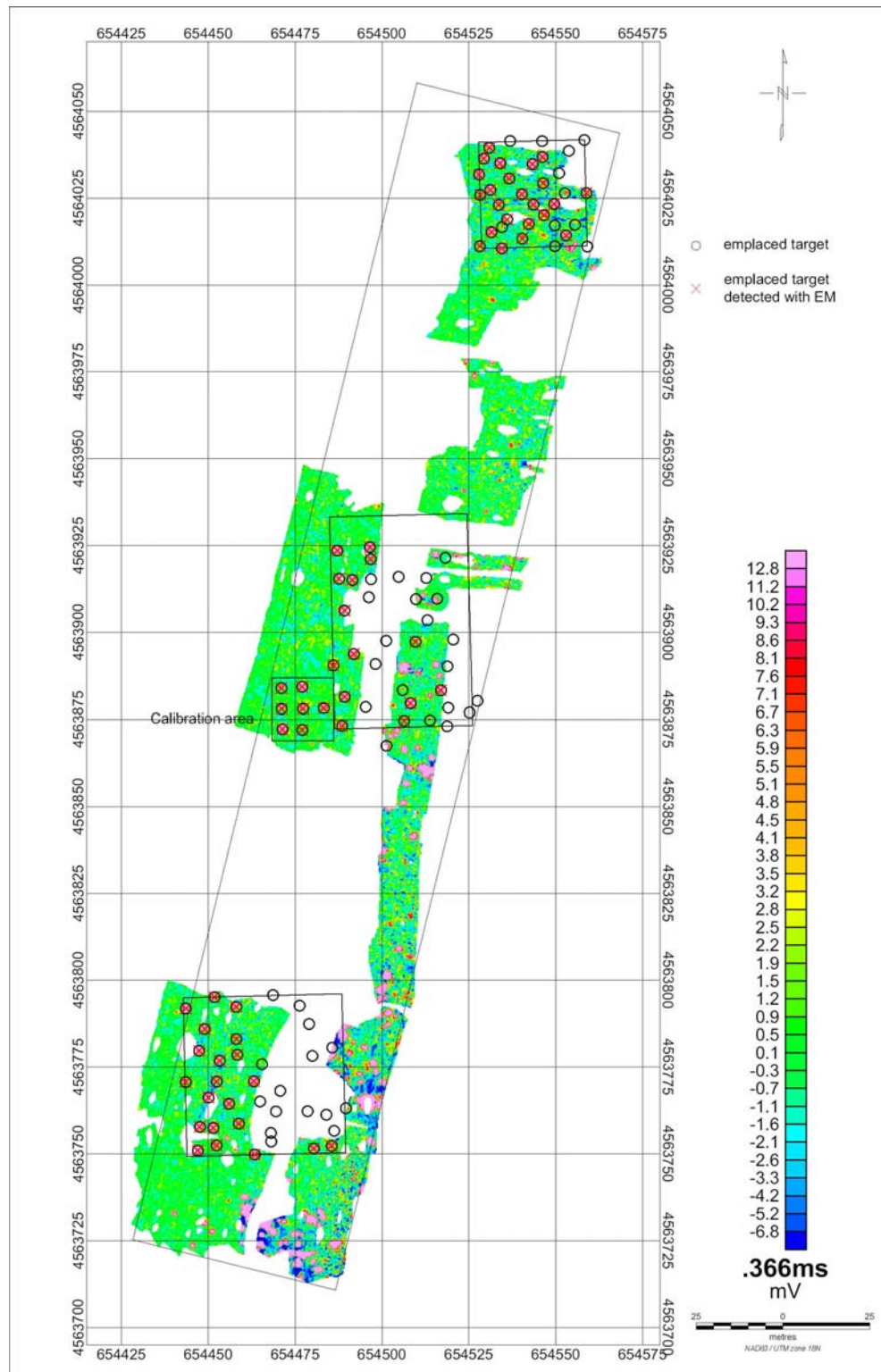


Figure 19. False color map showing the EMI data coverage overlain by locations of the emplaced targets and those declared detected during analysis.

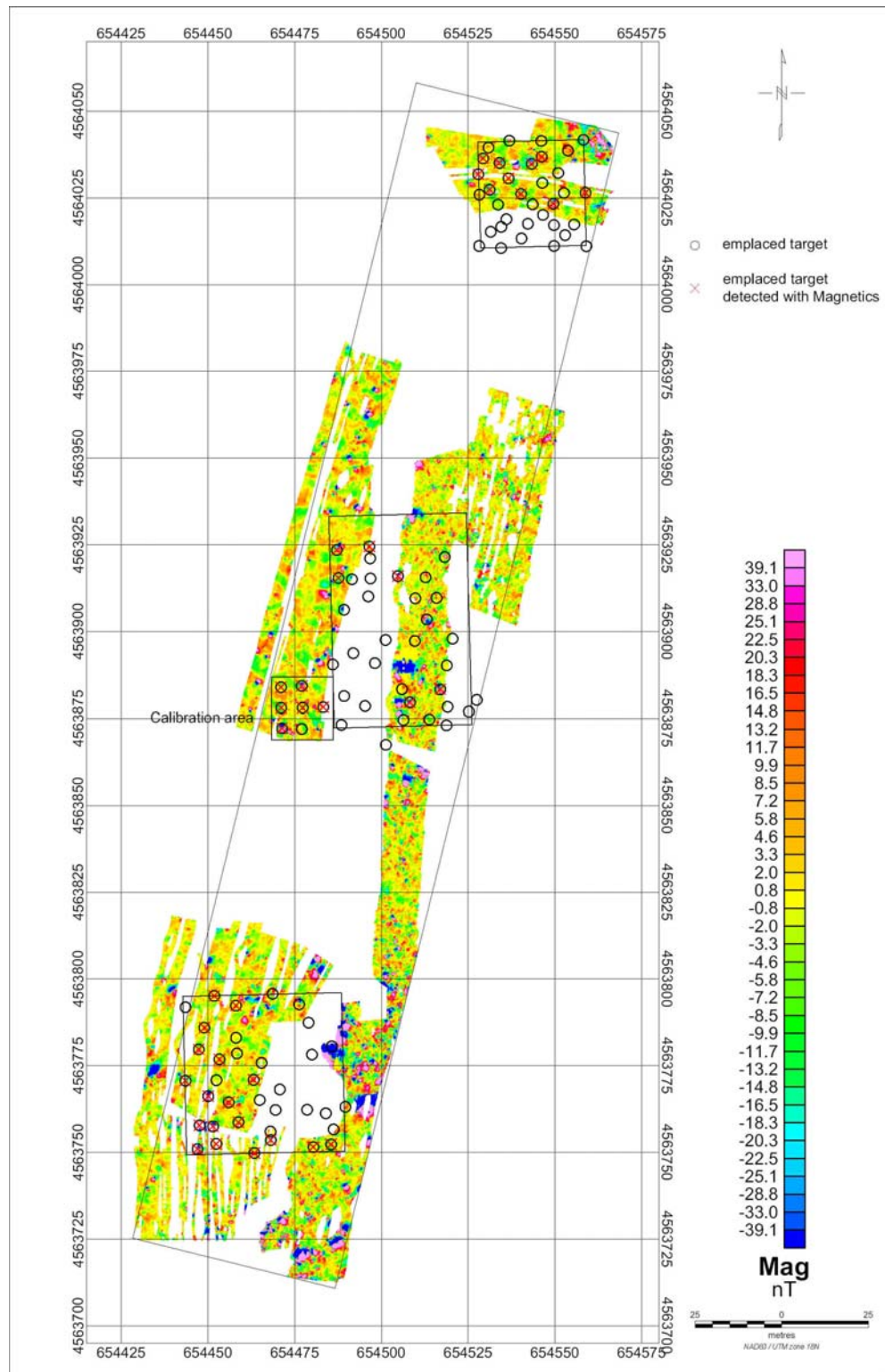


Figure 20. False color map showing the magnetic data coverage overlain by locations of the emplaced targets and those declared detected during analysis.

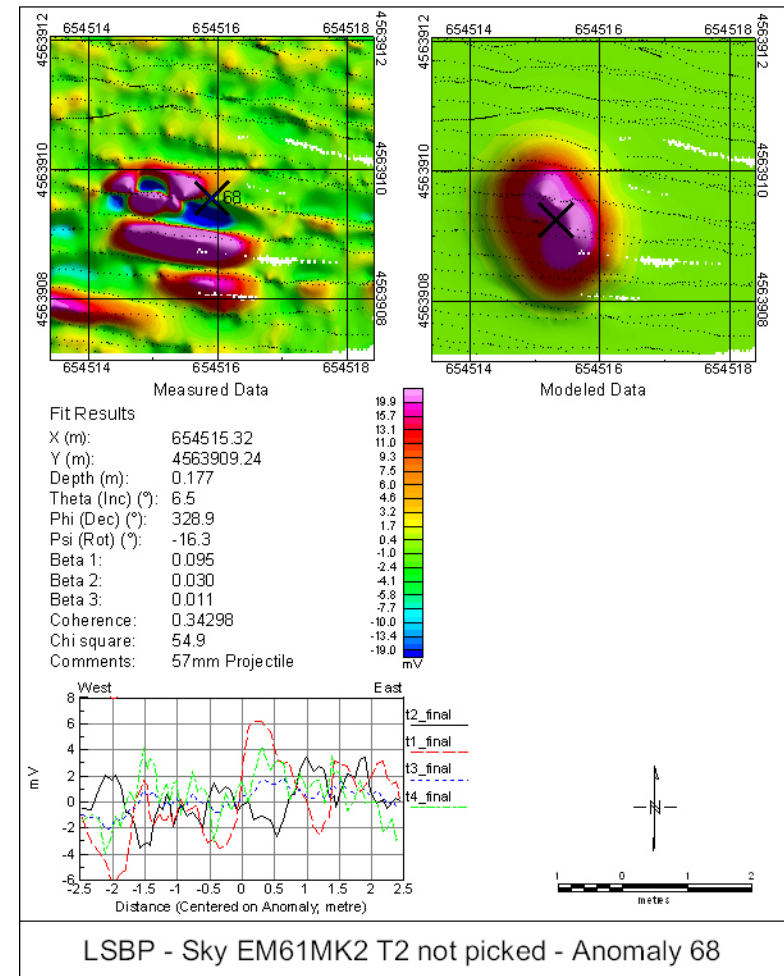
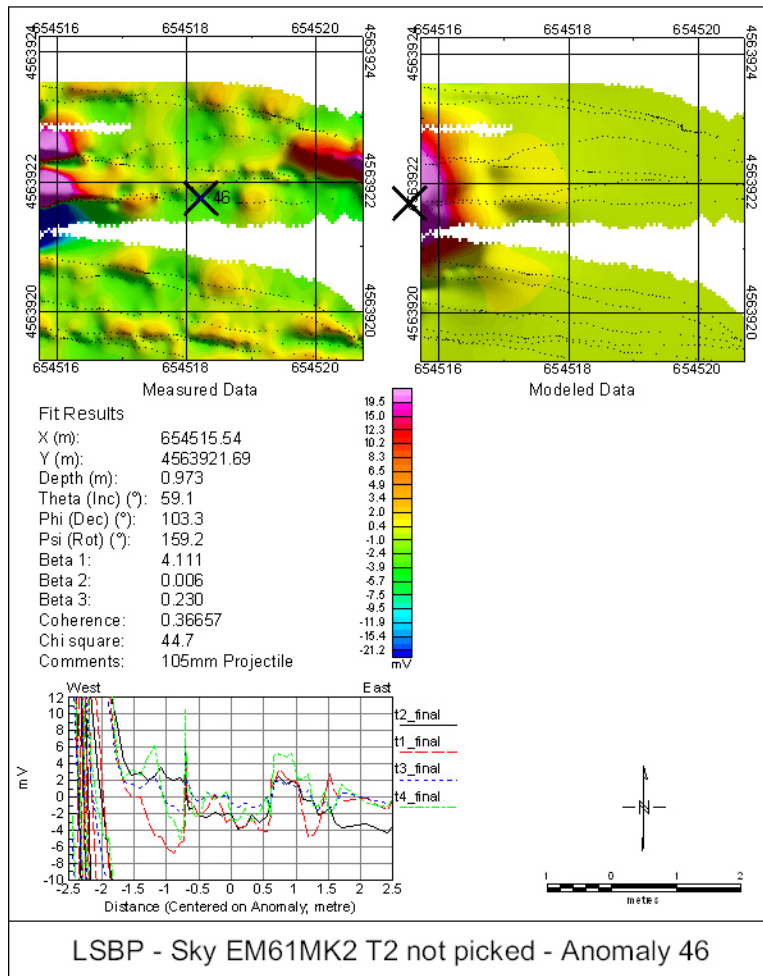


Figure 21. Anomaly plots of two emplaced targets that were not picked as targets in the EMI data. Left Anomaly Plot – The location of a 105mm projectile is identified by the cross in the upper left map, but no signature is observed. Right Anomaly Plot – The location of a 57mm projectile is identified by the “X” in the upper left map. The ‘Comments’ field, which is located just above the profile in the two plots, reports the UXO type from the ground truth information.



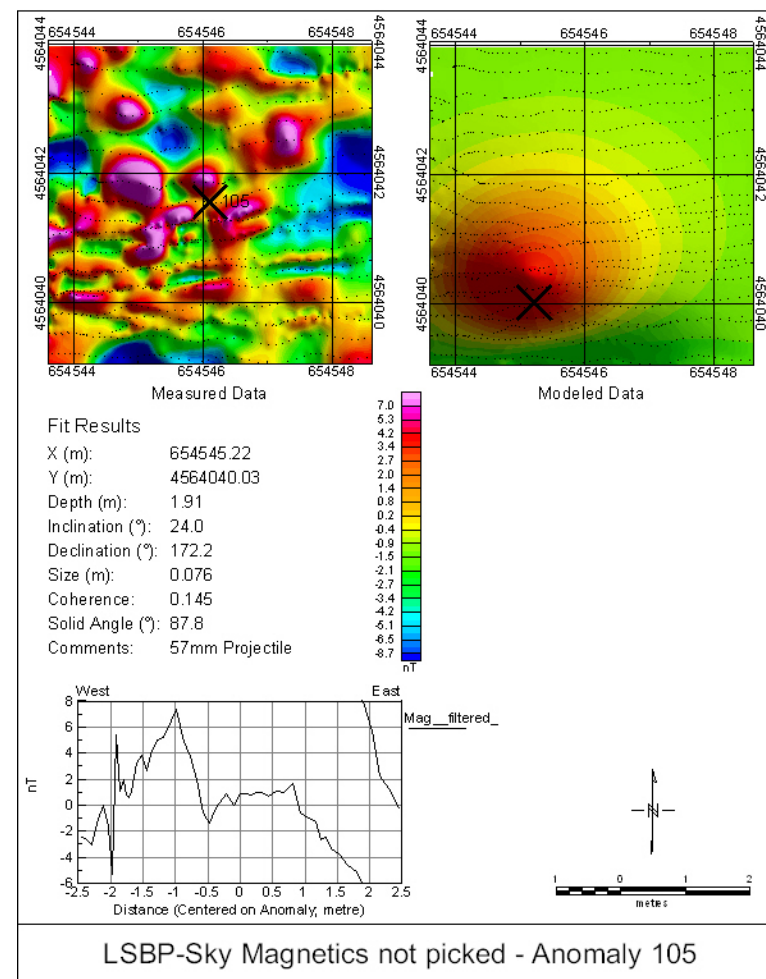
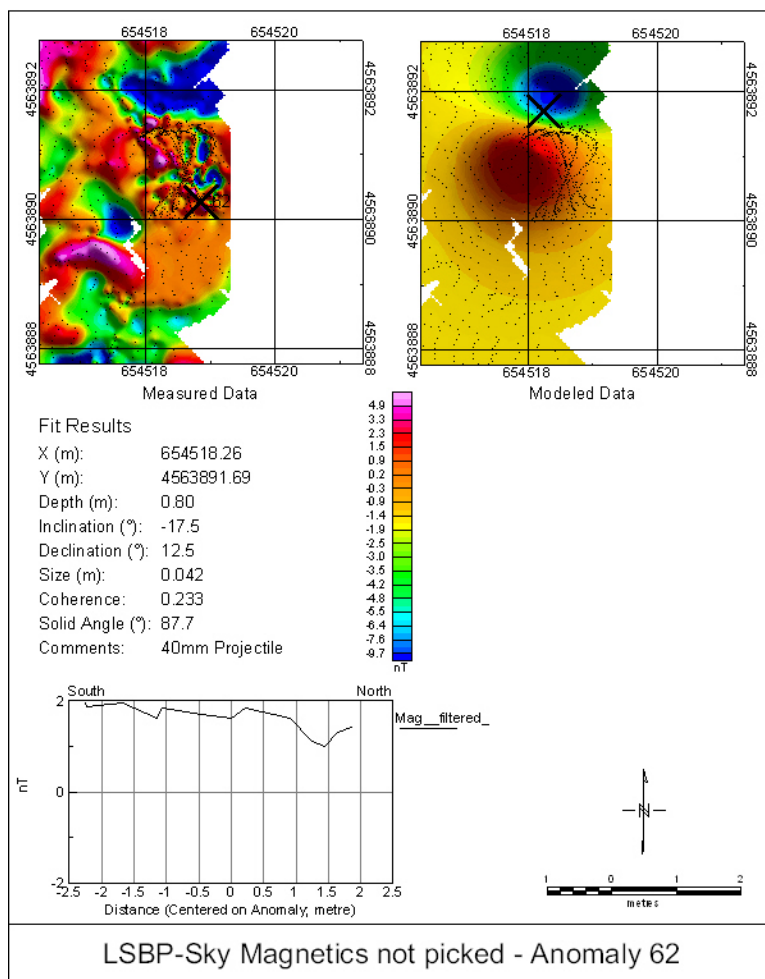


Figure 22. Anomaly plots of two emplaced targets that were not picked as targets in the magnetic data. Left Anomaly Plot – The location of a 40mm projectile is identified by the cross in the upper left map. The spatial sampling pattern shown in the plot presumably resulted from trying to push and twist the pushcart through the grasses and cut debris. Right Anomaly Plot– The signature of a 57mm grenade, identified by the “X” in the upper left map, is within the background noise. The ‘Comments’ field, which is located just above the profile in the two plots, reports the UXO type from the ground truth information.

## 4.3.2 Discrimination

### 4.3.2.1 Comparison of key Decision Metrics; Cued vs. Survey Data

Because emplaced UXO are symmetric and their shape is known and consistent, we can use them to evaluate the fitted parameters with respect to modeling errors and shape information. There are two fundamentally important measures. The first has to do with the ability of the inversion routine to reproduce the measured signal. In other words, how well does the modeled data match that which is measured? If the match is poor, the significance of the inverted source parameters is diminished. For this measure, we show the dipole fit error, defined as the square root of 1 minus the squared correlation coefficient between the measured and modeled data. The second measure relates to information regarding the estimated shape of the source object. For this measure, we utilize the absolute values of the three magnetic polarizability response coefficients.

A plot of fit errors versus maximum signal is shown in figure 23. In this figure, the red diamonds represent fitted parameters from the cued data and blue triangles identify survey data. The data shown here include only those emplaced objects that were surveyed using both acquisition approaches. As is clearly evident, the cued data possess higher amplitudes and significantly smaller fit errors than Sky's production survey.

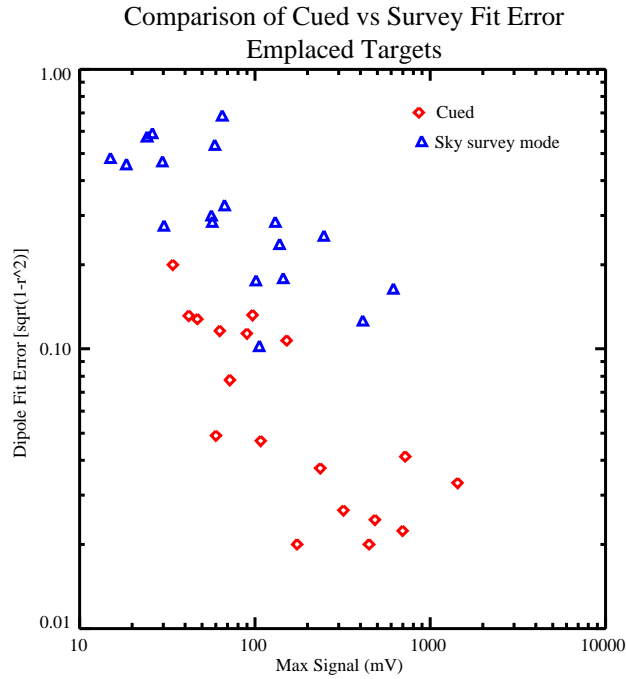


Figure 23. Scatter plot of the maximum signal versus dipole fit error. The data in this figure are restricted to emplaced UXO objects that were surveyed by Sky's production EM61 survey and the cued deployment.

As mentioned above, shape information can be a powerful discriminate metric if the aspect ratios and/or axial symmetry values of the UXO and clutter are separable. The three time-dependent dipole response coefficients relate to the principle axes of the target. The ratio of

the largest response coefficient to the mean of the remaining two, therefore, provides an estimate of the aspect ratio. Similarly, the two transverse response coefficients provide information about the axial symmetry. If the transverse coefficients are equal, the object can be thought to be axially symmetric.

Inverted shape measures for the emplaced targets are shown graphically in figure 24 and detailed in Table 5. In this figure, a log-log plot is used to visualize the feature space because of the tremendous range of values. The color-coded contours are derived from the test stand data and the symbols represent features derived from cued or survey data as indicated (each symbol represents fit results for one anomaly). The contours are centered about the mean measurement and extend two standard deviations for each ordnance type. Symbols on the y-axis are plotted at the average of the two smaller coefficients and the vertical line identifies the range. Plotted in this way, small vertical lines indicate axial symmetry.

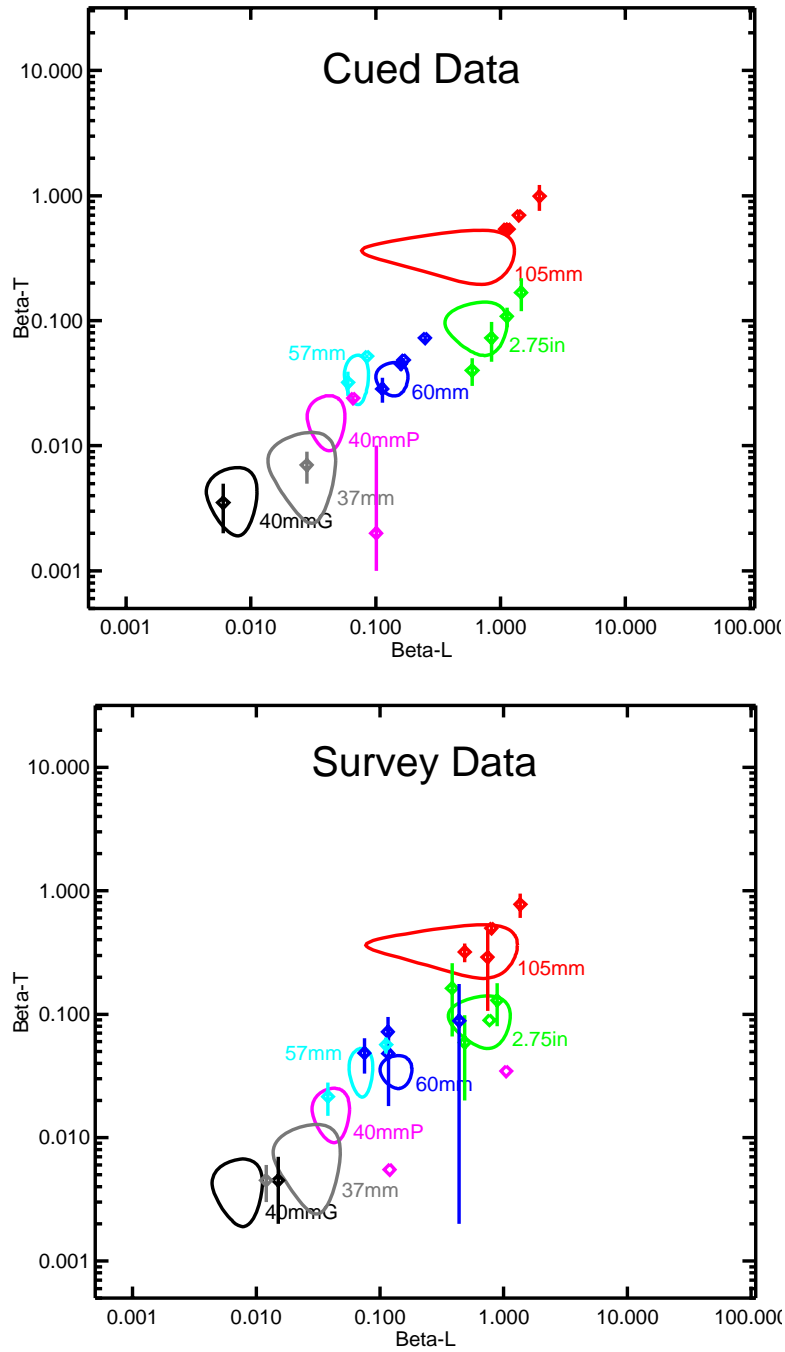


Figure 24. Magnetic polarizability coefficients for emplaced targets, EM61 MkII data, gate 2. For the transverse coefficients plotted on the y-axis, symbols identify the mean of the two smaller magnetic response coefficients and lines show the range.

Table 5 presents details regarding the derived shape indicators. Here, we list the dipole fit error, estimated aspect ratio, and an asymmetry metric for some of the emplaced UXO targets. The aspect ratio is derived by dividing the largest inverted response coefficient with the average of the smaller two.

As a rule, the estimated shape parameters from the cued data reproduced the measured signatures better than the survey data. The mean fit error, which is defined as the square root of 1 minus the squared correlation coefficient between the measured and modeled data, was 0.066 for the cued compared to 0.321 for the survey data.

The asymmetry metric is defined here as the difference between the two smaller response coefficients divided by the larger of the two. Expressed this way, the asymmetry metric ranges from 0 to 1, where 0 indicates that the two smaller response coefficients are equal and therefore axially symmetric and a value of 1 essentially indicates that the smaller response coefficient is equal to zero (to four decimal places). Remember that because the items included in this comparison are inert UXO, they all possess axial symmetry and ideally would result in asymmetry values of 0. As shown below, however, asymmetry values from the cued data show some scatter and a mean value of 25%. Asymmetry values from Sky's survey data possess considerably more variations and a mean value of more than 60%. Note that these asymmetry measures do not include the 40mm grenade because it is non-ferrous. Unlike ferrous objects, in which B1 is the largest with smaller and equal B2 and B3 values, non-ferrous objects have roughly equal B1 and B2 values and a smaller B3 value. Because of this, the asymmetry metric as defined here doesn't apply to the 40mm grenade.

Table 5. Fit Results for Emplaced Targets; Cued vs. Sky Survey Data

ID	Object	Burial Depth (m) (mid pt)	Cued Mode Fit Results				Survey Mode Fit Results			
			Fitted Depth (m)	Fit Error $\sqrt{1-(r^2)}$	Aspect Ratio [B1/avg(B2,B3)]	Asymmetry [(B2-B3)/B2]	Fitted Depth (m)	Fit Error $\sqrt{1-(r^2)}$	Aspect Ratio [B1/avg(B2,B3)]	Asymmetry [(B2-B3)/B2]
8	37mm	0.07	0.12	0.049	4.0	44%	0.01	0.469	2.8	55%
88	40mm Grenade*	0.09	0.03	0.128	1.7	60%	0.03	0.459	3.4	74%
94	40mm Projectile	0.12	0.14	0.047	2.8	8%	0.26	0.539	30.5	100%
100	57mm	0.08	0.05	0.024	1.6	7%	0.09	0.180	2.0	26%
103	57mm	0.22	0.19	0.132	1.9	36%	0.08	0.286	1.7	45%
43	60mm	0.32	0.30	0.132	4.0	37%	0.32	0.593	1.5	47%
107	60mm	0.10	0.10	0.020	3.4	6%	0.14	0.176	1.6	49%
108	60mm	0.14	0.15	0.037	3.5	20%	0.30	0.286	4.9	99%
110	60mm	0.22	0.31	0.107	3.4	9%	0.22	0.686	2.4	77%
9	105mm	0.18	0.25	0.033	2.0	13%	0.28	0.164	1.8	36%
10	105mm	0.23	0.32	0.022	2.0	11%	0.30	0.126	1.6	16%
11	105mm	0.49	0.57	0.020	2.1	5%	0.41	0.103	1.5	29%
47	105mm	0.57	0.77	0.077	2.1	38%	0.59	0.328	2.6	77%
80	2.75in	0.17	0.23	0.041	10.4	30%	0.22	0.254	6.8	55%
82	2.75in	0.31	0.35	0.026	11.7	52%	0.28	0.238	8.2	80%
84	2.75in	0.44	0.44	0.114	14.8	40%	0.53	0.301	8.6	100%
85	2.75in	0.64	0.72	0.116	8.7	45%	0.55	0.277	2.4	75%
MEAN			0.066				0.321			
STD DEV			0.045				0.170			

\* non-ferrous; not included in the mean and standard deviation asymmetry measures

As mentioned earlier, cued measurements were also taken for some native, non-emplaced targets. These targets were identified using data from an EM61 reconnaissance survey conducted by Foster Wheeler in 2000. The details of the source object were not known while selecting targets. Excavation results reveal that all of the native targets were clutter, some of which were axially symmetric.

Relevant data quality and shape metrics are presented in Table 6 for objects that were photographed, relatively isolated, and possessed acceptable signal to noise ratios. Representative photographs are shown in Figure 25. Once again, we look at data-model fit error, aspect ratio, and an asymmetry metric derived from the cued data as well as corresponding values derived from Sky's production data.

First, note that the fit error between the measured and modeled data for the cued approach is significantly smaller than the survey mode data. For these targets, the mean fit error for the cued measurements was 0.095 while the survey mode data had a mean fit error of 0.314. Second, note that with the exception of ID #14 (which was actually two moderately sized metallic fragments), the asymmetry values for those targets without axial symmetry (ID's 78 and 60) were greater than 50% for the cued data while those with axial symmetry (ID's 57,13,17,50, and 86) were not. If this 50% threshold is adopted, which is supported based on results from the emplaced targets (Table 5), the cued results would accurately predict symmetry for 12 of the 13 objects. As noted above, ID# 14 consists of two objects buried in close proximity, thereby violating the single-source assumption of the inversion routines. Three of the cued measurements (Id's 15, 55, and 51) possess asymmetry values greater than 100% because one or more of the inverted response coefficients for that target is negative.

Table 6. Fit Results for Native, Non-emplaced Targets; Cued vs. Sky Survey Data

ID	Photograph ID	Object	Axial Asymmetry	Cued Mode Fit Results			Survey Mode Fit Results		
				Fit Error $\sqrt{1-(r^2)}$	Aspect Ratio [B1/avg(B2,B3)]	Asymmetry [(B2-B3)/B2]	Fit Error $\sqrt{1-(r^2)}$	Aspect Ratio [B1/avg(B2,B3)]	Asymmetry [(B2-B3)/B2]
78	87	metal hinge	Yes	0.054	10.8	82%	0.438	2.8	58%
60	92	surface metal	Yes	0.070	1.8	68%	0.672	4.2	75%
14	253	2 metal pieces	Yes	0.057	10.7	22%	0.261	5.6	53%
	281	nails	Yes	0.221	3.9	81%	0.372	4.0	26%
15	276	nail and klinker	Yes	0.247	7.7	116%	0.327	4.0	55%
55	109	concrete slab	Yes	0.014	-1178.0	205%	0.178	6.3	100%
51	126	2"x14" flat steel bar	Yes	0.057	-2.1	-568%	0.385	4.4	100%
57	104	1" steel pipe in concrete	No	0.014	4.3	40%	0.281	3.2	100%
13	261	surface metal	No	0.050	13.6	33%	0.302	7.0	100%
17	327	rebar	No	0.157	3.5	40%	0.320	3.2	29%
50	387	oil filter	No	0.000	1.5	35%	0.126	2.4	28%
200	356	20in steel rod	No	0.178	4.1	36%	0.267	4.4	79%
86	463	6in metal chain	No	0.118	3.2	50%	0.150	6.4	74%
<b>MEAN</b>				<b>0.095</b>			<b>0.314</b>		
<b>STD DEV</b>				<b>0.081</b>			<b>0.141</b>		





Figure 25. Photographs of native, non-emplaced objects for which data was acquired using a cued deployment and production survey. The photograph ID numbers correspond to those listed in Table 6. Although difficult to read, the top left photo is ID 87.



#### 4.3.2.2 Cued data Discrimination Performance

Receiver operating characteristic curves for all (emplaced and native) cued data are shown in Figure 26. In this case, a GLRT classifier was trained and tested on the same set of features derived exclusively from cued data. As such, it presents the best case scenario given these cued measurements.

The graph on the left shows performances if we define the target of interest as UXO. The graph on the right presents performance if we define our target of interest as being symmetrical regardless of its classification of UXO. In these graphs, the ‘B1 B2 B3’ descriptor indicates the three response coefficients (eigenvalues of the magnetic polarizability tensor) directly. The term ‘asymmetry’ and ‘aspect ratio’ were defined as before (i.e., see Table 6).

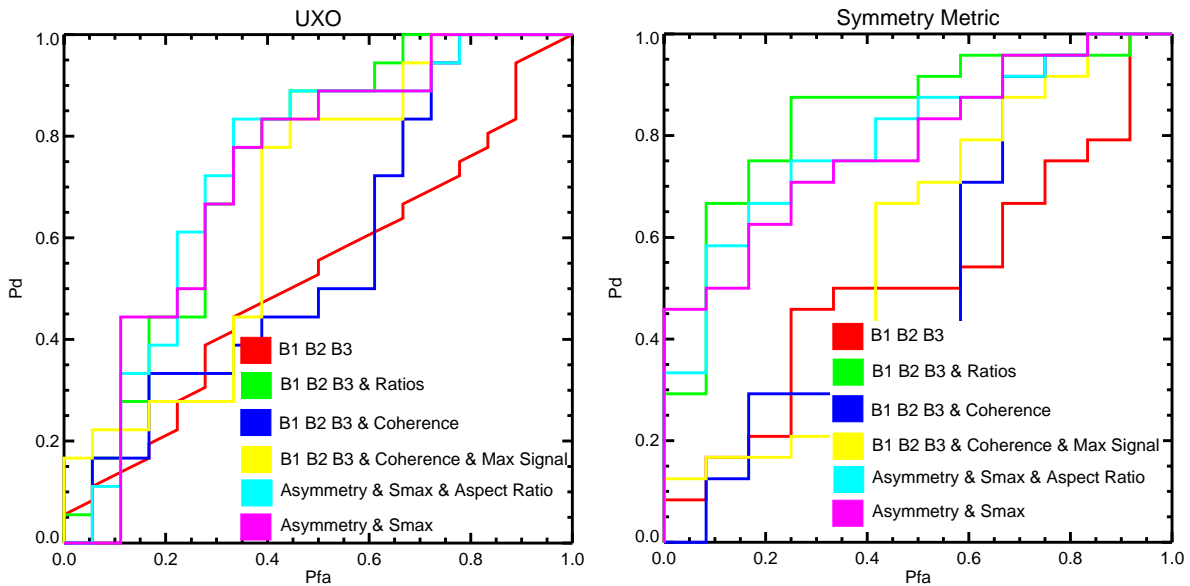


Figure 26. Receiver operating characteristic curves for cued data only.

#### 4.3.2.3 Controlled Test Measurements

For comparison purposes, Table 7 presents estimated shape information as derived from the test stand data. In this table, the mean value and standard deviation are reported for the coherence, estimated aspect ratio, and estimated asymmetry. Statistical measures are reported because the test stand protocol included recording data for each item at six discrete orientations relative to the sensor coil. The sensor-ordnance orientations were nose up, nose down, horizontal along the X-axis, horizontal along Y-axis, 45-degree nose up, and 45-degree nose down. The ordnance objects were positioned such that the signal strength was as strong as possible without saturating the analog-to-digital converter. A couple of interesting notes are apparent. First, by looking at the fit errors, it is clear that the inversion process reproduced the measured data very well. Second, and perhaps most importantly, the mean asymmetry values for emplaced, symmetrical UXO is 15% compared to 25% for the cued and 60% for Sky’s survey data (Table 5). In other words, the inverted shape parameters

more accurately and consistently reflect axial symmetry than either the cued or production survey data.

Table 7. Fit Results for Emplaced Targets; Test Stand Data

Object	Test Stand Fit Results					
	Fit Error $\sqrt{1-(r^2)}$		Aspect Ratio $[B1/\text{avg}(B2,B3)]$		Asymmetry $[(B2-B3)/B2]$	
	Mean	Std Deviation	Mean	Std Deviation	Mean	Std Deviation
37mm Projectile	0.068	0.017	3.8	0.69	10%	5%
40mm Grenade	0.199	0.023	1.7	0.30	33%	14%
40mm Projectile	0.090	0.051	2.5	0.56	13%	7%
57mm Projectile	0.052	0.028	1.9	0.32	9%	5%
60mm Projectile	0.036	0.017	3.8	0.57	11%	6%
105mm Projectile	0.019	0.009	1.9	0.62	6%	3%
2.75in Rocket	0.020	0.013	7.4	1.38	22%	17%
<b>MEAN</b>	<b>0.069</b>				<b>15%</b>	

#### 4.3.2.4 Sky EM61 Survey Data

A total of 150 anomalies were identified in the production EMI data (shown in Figure 19) and inverted for model parameters. The model parameters were classified using a support vector machine (SVM). The features used by the SVM classifier were (i) the estimated size, (ii) the two smaller response coefficients, and (iii) coherence. For this effort, we ranked the classifier outputs using a scheme of 1, 2, and 3, where a rank of 1 indicates high confidence UXO, rank 3 is used for high confidence clutter, and rank 2 is everything else. The rankings were selected after plotting the classifier outputs in descending order and superimposing classifier outputs for the seven calibration targets (Figure 27). A threshold of 0.25 was selected to separate rankings 1 and 2, and a threshold of -0.2 was used to segment rankings of 2 and 3. The later threshold was partially based on the slope change in the classifier output.

Results of the classification reveal that of the 58 seeded items, 41 were ranked as high confidence ordnance rank 1, 10 were ranked as high confidence clutter rank 3, and 7 remained unclassified (rank 2). Figure 28 presents a receiver operating characteristic curve. From the ROC, we see that the % UXO correctly classified is 0.74 (viz., the Pd for rank 1) and the False Alarm metric is 0.15 (1-Pd for rank 3 anomalies). Note that the ROC includes results for the seven calibration targets that were within the survey area.

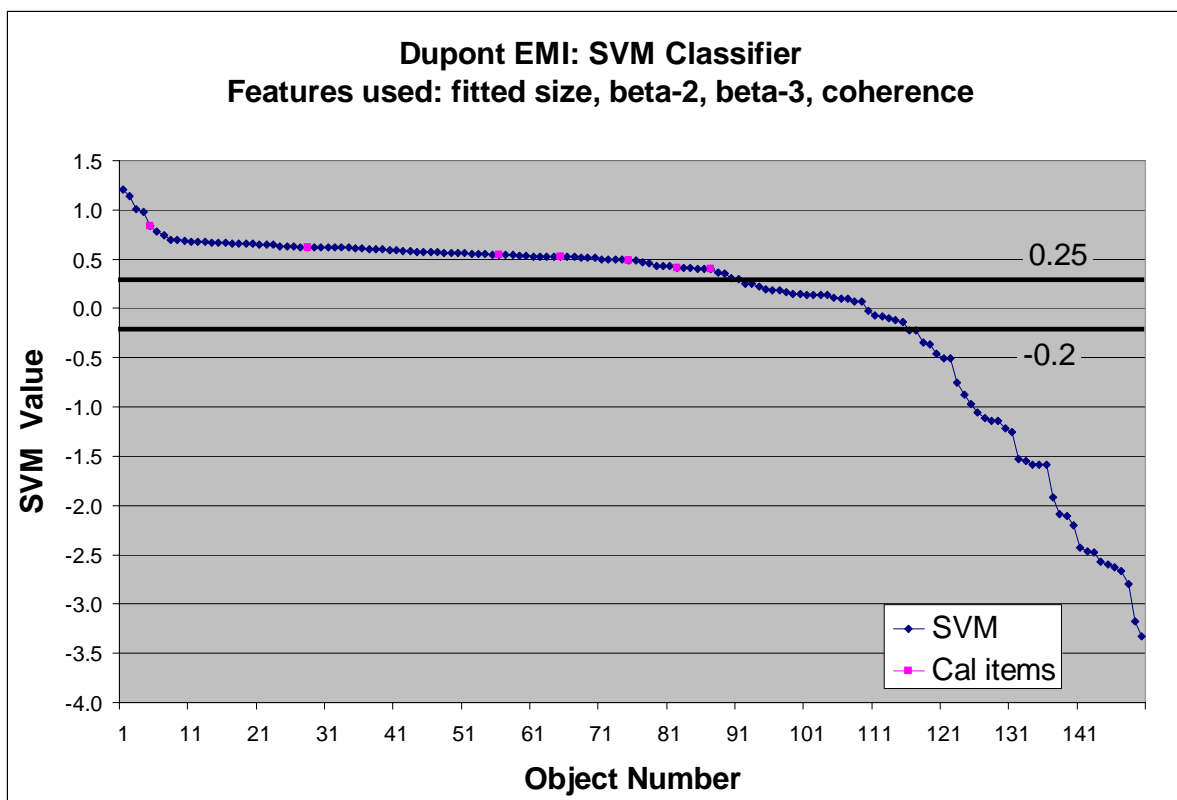


Figure 27. Output from Duke's Support Vector Machine classifier; Sky's EM61 data. Each point represents the classifier value for an individual anomaly. The magenta symbols identify inert UXO items buried within the site which were used for calibration purposes.

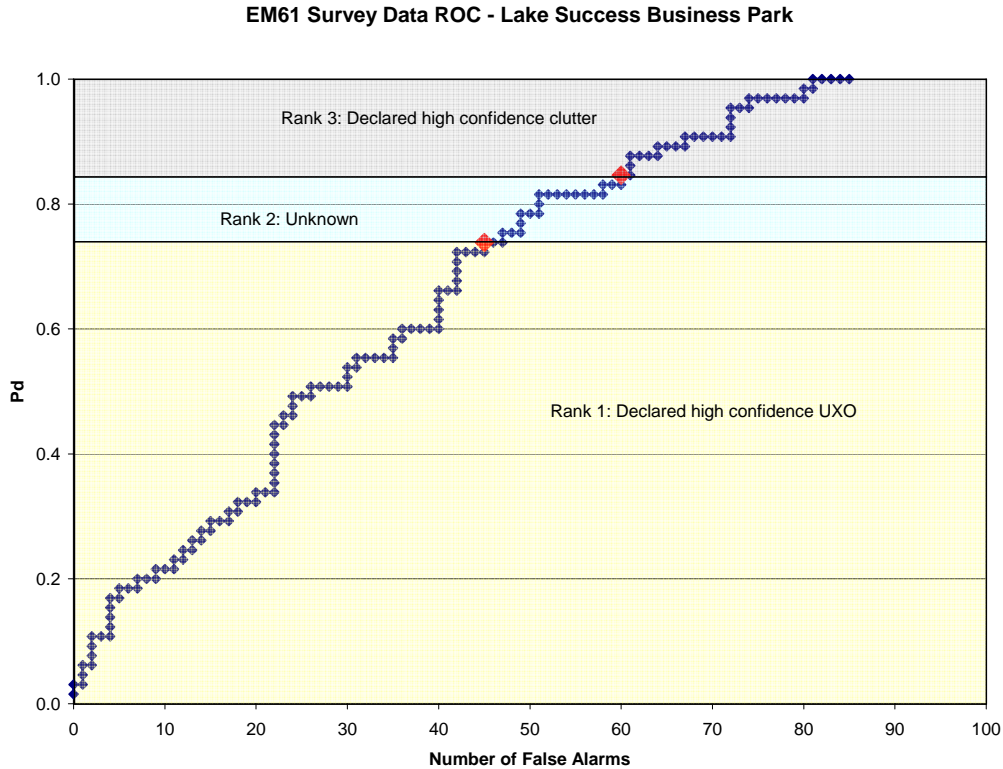


Figure 28. Receiver operating characteristic curve for EMI classifications. The blue symbols plot  $P_d$  as a function of the number of false alarms. The red diamonds identify thresholds between rankings.

#### 4.3.2.5 Observed Fit Errors; dynamic versus static surveying

For comparison purposes, Figure 29 overlays the model fit errors for data acquired in a moving, dynamic sensor platform (Sky's EM61 survey data) with those associated with a non-moving, stationary sampling scheme (cued and test stand data). As clearly observed here, the fit errors for the dynamic survey are significantly larger than either of the non-moving acquisition modes. Note that although most of the cued results are grouped with the test stand results, some are mingled with the survey fits. After investigating, we find that larger fit errors for the cued data were caused by overlapping signatures or were associated with low amplitude responses.

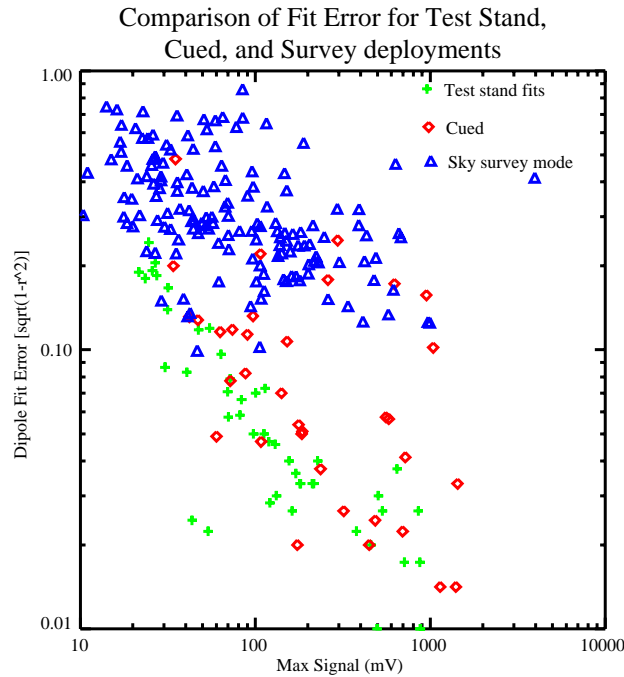


Figure 29. Scatter plot of the maximum signal versus dipole fit error for the test stand measurements, all cued targets (emplaced and non-emplaced), and all anomalies detected in Sky's EM61 MKII survey.

#### 4.3.3 Depth Estimates

Comparisons of the actual versus fitted depth are shown in Figure 30 for cued and survey mode EMI data. The top plot shows results for all of the emplaced targets regardless of the fit error between measured and modeled data. As anticipated, the cued data depth estimates show less scatter and better match actual depths than the survey data. The bottom plot only includes results for objects that possess a fit error of less than 0.22 (selected here for illustrative purposes). Comparing the two plots, we see that all of the cued features remain but a significant number of the survey data features were removed. In fact, the mean fit error for cued data collected over the emplaced UXO was 0.09 compared to 0.37 for the survey data. Also note that most of the cases above this threshold also had inaccurate depth estimates.

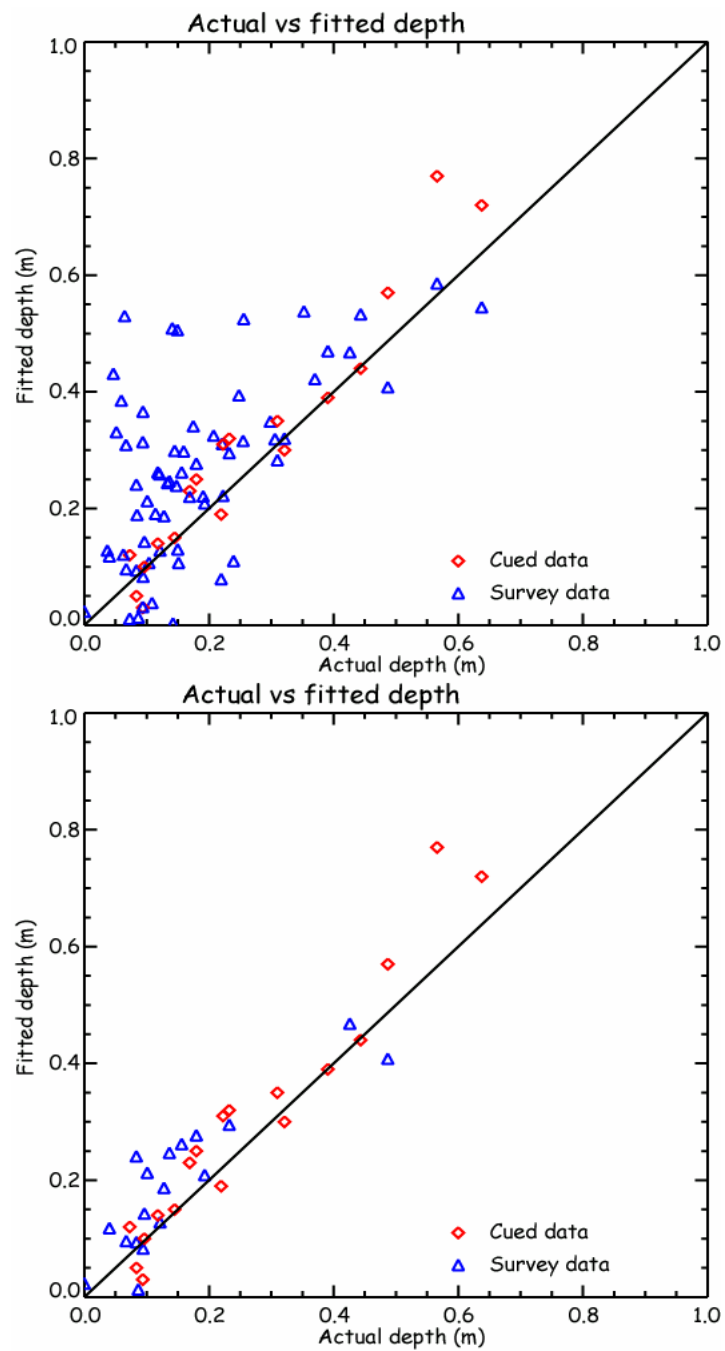


Figure 30. Actual versus fitted depths for emplaced targets. Top: all seeded items, bottom: results for anomalies that possess fit errors of less than 0.22.

#### 4.3.4 Qualitative Metrics

UX-Analyze characterizes and classifies individual anomalies. Steps taken within the characterization phase include identifying anomalies, selecting the spatial footprint of the anomaly, and reviewing the results. The most labor intensive portion of the characterization phase is identifying the spatial extent of each anomaly and editing individual samples that are inconsistent. UX-Analyze provides graphical presentations and appropriate tools to assist the analyst. Once completed, individual anomalies are inverted manually or in batch mode. The output of the characterization phase is a list of model parameters for each anomaly which is then submitted to the classifier. Steps taken during the classification phase include creating or updating a library for training purposes, selecting and calling the classifier.

UX-Analyze adheres to the look and feel of Oasis montaj and, as such, is quickly mastered by experienced Oasis montaj users. It is easy to use and includes an on-line help menu. During this demonstration, Oasis montaj underwent a number of major upgrades that affected the performance and robustness of UX-Analyze. These coding inconsistencies have been corrected. As of this report, January 2007, the current Oasis montaj release is 6.4, and we do not experience systematic difficulties while processing and analyzing these magnetic and EMI data.

#### 4.4 Discussion

The feature-based EMI characterization approach demonstrated here inverts measured EM61 field data assuming a point dipole source and then separates the targets into classes using the model parameters. The derived model parameters are meaningful, however, only if the modeled data accurately represent the measured data. In other words, the dipole fit error, or the difference between the measured and modeled data, must be insignificant. We have found through experience that if the fit errors are greater than 0.1, the recovered parameters are often inaccurate.

Unfortunately, the mean fit error for EM61 survey data acquired during this demonstration is 0.3 or larger (survey mode emplaced targets only; Table 5). In other words, for the average anomaly, only 70 percent of the measured data is explained by the model. Because of this, little confidence can be placed in the inverted features. These EM61 survey data, which were spatially registered using a laser based robotic total station, do not support feature based decisions.

In contrast to the survey data, the cued measurements produced data that was well modeled using a dipole source. On average, the inversion process accurately accounted for over 94% of each cued anomaly data. Even given the good model fits, however, perfect classification isn't guaranteed. For these cued data, the discrimination performance is along the chance diagonal if the inverted, intrinsic shape parameters (viz., the three response coefficients) are used to classify targets as UXO or not (Figure 26). Performances are improved, but not yet ideal, if we classify using ratios of the betas, axial asymmetry and/or aspect ratio estimates.



Additional performance gains are realized if we decide that our target of interest includes axially symmetric metallic objects as well as UXO.

## **5. Cost Assessment**

### **5.1 Cost Reporting**

<b>Cost Category</b>	<b>Sub Category</b>	<b>Costs</b>
Data Acquisition	Site Visit, Equipment Prep and Survey	\$40,000
Data Characterization and Classification	Anomaly Specific Characterization 250 @ \$6 per anomaly	\$1,500
	Anomaly Plots 250 @ \$0.05 per anomaly	\$15
Reporting	Analysis & Final Report	\$60,000

### **5.2 Cost Analysis**

The major cost components of this demonstration acquiring the data, making sense of the results, and compiling the report. A non-trivial amount of labor and effort was exerted trying to acquire high-fidelity data that would support feature-based analysis, process the data once acquired, and to extract all possible information from the signatures. As shown above, the data characterization and classification tasks were not major contributions to the project costs.

## **6. Implementation Issues**

### **6.1 End User Issues**

The primary end-users of this data analysis technology will likely be high-end geophysical service providers, technically savvy DoD oversight personnel, and government-sponsored researchers. As demonstrated here, however, feature-based discrimination decisions require geophysical data that have high signal-to-noise ratios, are isolated, and possess high spatial registration precision.

## 7. References

Ambrose, B., Bell, T., and Furuya, T., March 2004, UXO clearance at the Lake Success Redevelopment Project, Department of Defense UXO/Countermines Forum.

Barrow, B., and Nelson, H., 1998, *Collection and Analysis of Multi-sensor Ordnance Signatures with MTADS*, J. Environ. Engineering Geophysics, **3**, p. 71.

Barrow, B., and Nelson, H., 2001, *Model-based Characterization of Electromagnetic Induction Signatures Obtained with the MTADS Electromagnetic Array*, IEEE Transactions On Geoscience Remote Sensing, **39**, p 1279-1285.

Bell, T., Barrow, B., and Miller, J., 2001, *Subsurface Discrimination using Electromagnetic Induction Sensors*, IEEE Transactions On Geoscience Remote Sensing, **39**, 1286-1293.

Department of Defense, March 2001, *Unexploded Ordnance Response: Technology and Cost*, Report to Congress.

ESTCP Cost and Performance Report 199526, *Multi-sensor Towed Array Detection System*, <http://www.estcp.org/documents/techdocs/199526.pdf>.

Robitaille, G., Adams, J., O'Donnell, and Burr, P., 1999, *Jefferson Proving Ground Technology Demonstration Program Summary*, <http://aec.army.mil/usaec/technology/jpgsummary.pdf>.

Section 349 (Public Law 105-85), Partnerships for Investment in Innovative Environmental Technologies.

Senate Report 106-50, National Defense Authorization Act for Fiscal Year 2000, May 17, 1999.

Research and Development to Support UXO Clearance, Active Range UXO Clearance, and Explosive Ordnance Disposal, p 291–293.

## 8. Points of Contact

### **ESTCP**

Anne Andrews

ESTCP  
901 North Stuart Street  
Suite 303  
Arlington, VA 22203

Tel: 703-696-3826  
Fax: 703-696-2114  
Anne.Andrews@osd.mil

Program Manager  
UXO Thrust Area

Jeffrey Fairbanks

HydroGeologic, Inc.  
1155 Herndon Parkway  
Suite 900  
Herndon, VA 20170

Tel: 703-736-4514  
Fax: 703-471-4180  
jef@hgl.com

Program Assistant  
UXO Thrust Area

### **SAIC**

Dean Keiswetter

SAIC  
120 Quade Drive  
Cary, NC 27513

Tel: 919-653-0215  
Fax: 919-653-0219  
dkeiswetter@nc.aetc.com

PI

Tom Bell

SAIC  
1225 Jefferson Davis Highway  
Suite 800  
Arlington, VA 22202

Tel: 703-413-0500  
Fax: 703-413-0512  
tbell@va.aetc.com

Co-PI

Tom Furuya

SAIC  
120 Quade Drive  
Cary, NC 27513

Tel: 919-653-0215  
Fax: 919-653-0219  
tfuruya@nc.aetc.com

Data Analyst

### **Dupont**

Brian Ambrose

DuPont Engineering  
Barley Mill Plaza, Bldg 27  
Wilmington, DE 19880

Tel: 302-992-5869  
Fax: 302-992-4869  
Brian.Ambrose@usa.dupont.com

Senior Health &  
Safety Specialist